CHARACTERIZATION OF POLARIZATION DEPENDENT LOSS IN OPTICAL FIBRES AND OPTICAL COMPONENTS IN THE PRESENCE OF POLARIZATION MODE DISPERSION

by

Gaoboelwe Pelaelo

Submitted in partial fulfilment of
the requirements for the degree of

MAGISTER SCIENTIAE

in the Faculty of Science
at the Nelson Mandela Metropolitan University

Supervisor: Professor A.W.R. Leitch
Co-supervisor: Doctor L. Wu

January 2008

To my family and friends

Acknowledgements

- My sincere gratitude to my supervisor, Prof A W R Leitch and my co-supervisor, Dr L Wu for all their support and guidance throughout this study

- Dr T Gibbon for fruitful discussion in my research

- I would like to thank members of the fibre optic research group for their enthusiasm and encouragement of my research

- I wish to thank the staff at Telkom (Port Elizabeth) for their patience and the time they have given us to perform measurements

- The support and guidance I got from all other members of the physics department is well appreciated

- I wish to thank NMMU and Arberdare Fibre Optic Cables, Corning Optical Fibre, Telkom, THRIP, MCT TELECOMMUNICATIONS, as well as INGOMA communication services for their financial support

- My family and friends for their continual support throughout my studies

CONTENTS

SUMMARY

In this study, the Jones matrix eigenanalysis (JME), optical spectrum analyzer (OSA) and polarization scrambling methods were used to investigate polarization dependent loss (PDL) in the presence of polarization mode dispersion (PMD) in optical components and fibres. The PDL measurements were conducted both in the laboratory and in the field. For field measurements, a buried link (28.8 km) and an aerial fibre (7.1 km) were extensively studied. The findings obtained from these studies are very important for network operators who must assess the impact of PDL on the network reliability.

The three different PDL measurement methods (JME, OSA and polarization scrambling) were compared and their PDL values were found to agree very well at the selected wavelength of 1550 nm. Concatenation of PDL components showed that as expected, PDL increase as the number of PDL components were added.

The interactions between PMD and PDL measurements were analyzed. A PMD/PDL emulator was constructed. We observed that PMD decreased while PDL increased. The PMD decrease was a result of the PMD vector cancellation enhanced by the randomly distributed mode coupling angles while PDL increase was a result of each PM fibre segments contributing to the overall global PDL. It was observed that the presence of PMD in a link containing PDL, results in PDL being wavelength dependent and this resulted in the extraction of the PMD information from the PDL data. PDL was found to be Maxwellian distributed when considering low values of PMD. High PMD values resulted in the PDL distribution deviating from Maxwellian. Long-term PDL and PMD (average DGD) measurements indicated that the PDL and PMD varied slowly with time and wavelength for both the laboratory and field measurements. It was observed that the BER increase as both PDL and PMD increased for simulated optical link.

***Keywords**: JME, optical fibre, OSA, polarization dependent loss, polarization mode dispersion and polarization scrambling.*

ABBREVIATION LIST

BER bit error rate

DGD differential group delay

DOP degree of polarization

DUT device under test

DWDM dense wavelength division multiplexing

EDFA erbium doped fibre amplifier

IL insertion loss

JME Jones matrix eigenanalysis

NRZ non-return to zero

ORL optical return loss

OSA optical spectrum analyzer

OSNR optical signal to noise ratio

PRBS pseudorandom bit sequence

PDF probability density function

PDL polarisation mode dispersion

PMD polarization mode dispersion

PMF polarization maintaining fibre

PSA Poincare sphere analysis

PSP principal states of polarization

SMF single mode fibre

SOP state of polarization

WDM wavelength division multiplexing

CHAPTER 1

INTRODUCTION

Communication and access to information are the basic needs of human beings for a successful and better growth of economy. This forms part of a person's interaction in the modern society, sending messages from one distant area to another. The everyday bandwidth consumption has resulted in the emergence of new technologies such as wavelength division multiplexing (WDM) and dense wavelength division multiplexing (DWDM) in the telecommunication fields. These technologies incorporate a great number of optical components. Examples are isolators, splitters, WDM multiplexers/demultiplexers, amplifiers, polarizers and circulators which form part of the backbone in the transmission networks. These components as well as the optical fibre are polarization sensitive; as such they exhibit polarization dependent loss (PDL) and polarization mode dispersion (PMD). These two polarization effects are problematic especially at high bit rates, 10 Gb/s and above, which has resulted in another area of extensive research for telecommunication operators and scientists.

Besides PDL, the insertion loss (IL) and optical return loss (ORL) are other major losses that degrade the transmitted signal. Characterization of optical components for ORL and IL is critical for ensuring optimum performance in telecommunication networks. Most of the optical components exhibit insertion loss of greater than 3 dB and optical return loss of greater than 50 dB. It is therefore important to measure and control these losses (IL and ORL) during research, development and deployment. A few example measurements to illustrate the IL and ORL of optical components are presented in Chapter 2.

PDL is determined from the maximum and minimum ratio of the output power when the component is exposed to different states of polarization (SOPs). PDL is known to degrade signal to noise ratio (SNR) due to the increased power fluctuation and consequently, higher bit-error rate (BER) which degrades the transmission system. PMD is caused by the non-circularity of the fibre core which induces fibre birefringence. This results in a differential group delay (DGD)

between two polarization modes of the transmitted signals, which causes optical pulse broadening and consequently signal distortions.

The combined PMD and PDL cause severe effects which totally limit the transmission systems. At high bit rates, ≥10 Gb/s, these polarization effects limit the transmission networks by increasing the BER. When combined with PMD, PDL changes with time and wavelength, therefore requires a statistical description. It is therefore important to characterize and compensate these effects to improve the system performance.

To this end, the work presented in this dissertation is organized as follows: Chapter 2 deals with the aspects relating to some of the losses encountered in telecommunication networks. Chapter 3 introduces the theory behind PDL and PMD. Their definitions, origins and their combined effects are outlined. Chapter 4 discusses some of the recent work on PDL in the presence of PMD by various researchers.

Chapter 5 is dedicated to a discussion of PMD and PDL measurement techniques. A number of PDL measurement techniques are provided and discussed, namely, Jones matrix eigenanalysis (JME), Mueller matrix (MM), optical spectrum analyzer (OSA) and the polarization scrambling methods. Their theoretical background and experimental setups are shown.

Chapter 6 provides PDL results obtained using three different techniques (JME, OSA and polarization scrambling methods). The PDL results from the three techniques are then compared. In addition, results on the interaction of PDL and PMD are presented. Simulated bit error rate (BER) on the influence of PDL and PMD values is obtained by using Virtual Photonics Transmission Maker 7.5. Chapter 7 presents the conclusions of the important findings of this work.

Chapter 2

Losses in optical components and fibres

This chapter gives a brief overview on losses encountered in optical fibre communication systems. Losses induce signal distortions that limit the information carrying capacity of a fibre. By quantifying these losses in fibre communication systems the maximum distance between a transmitter and a receiver can be determined. The insertion loss (IL), optical return losses (ORL) and polarization dependent losses (PDL) in optical components and fibres will be covered. As insertion loss and optical return loss are not a major focus of this dissertation, a few example measurements to illustrate IL and ORL will be included in this chapter.

2.1. Insertion loss (IL)

The light that is transmitted through a fibre can be absorbed, scattered and reflected by an optical component. Insertion loss (IL) determines how much light is transmitted through a component. This is the ratio of the incident power to the transmitted power for a component. IL is one of the important parameters to measure in dense wavelength division multiplexing (DWDM) systems. This parameter determines the network's power budget calculation, and so every component has to be quantified for insertion losses.

The insertion loss is defined by the telecommunication standards such as TIA/EIA-455-157:

$$IL = 10 \times \log\left(\frac{P_{incident}}{P_{transmitted}}\right) \tag{2.1}$$

where $P_{incident}$ and $P_{transmitted}$ refers to the incident and transmitted power to the component under test. It is expressed in logarithm scale in units of decibels (dB) and it is positive since the incident power will always be higher than the transmitted power.

To determine the insertion loss of an optical component the procedure below is followed:

1) The power incident on the device under test (DUT), $P_{incident}$, is measured by connecting the optical source directly to the power meter using a reference fibre.
2) The transmitted power, $P_{transmitted}$, through the DUT is then recorded using the power meter.

Figure 2.1 shows the instrumental set-up required for insertion loss measurements of optical devices.

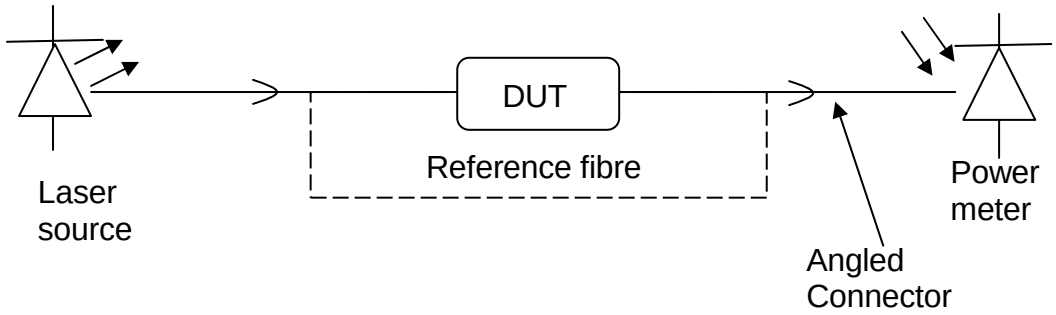

Figure 2.1: Measurement set-up for insertion loss

The uncertainties in the insertion loss measurements are due to connectors in the set-up. Their losses change when they are disconnected and reconnected. To ensure accurate measurements, the DUT is spliced into the setup and the DUT measurement is recorded first. The DUT is then excluded from the signal path and the splice that induced additional losses is kept in the setup. The incident power is then measured. The reference measurement allows one to capture the induced splice loss (Application note[1]). Other sources of uncertainty include unstable input power from short-term fluctuations of the source due to multiple reflections. In addition, changes in the input state of polarization (SOP) can lead to varying insertion loss due to polarization dependent loss of the device.

Figure 2.2 shows the insertion loss measurement conducted on a 50:50 beam splitter. The insertion loss was calculated from the difference between the averages of the reference power and the measured power after the DUT was inserted.

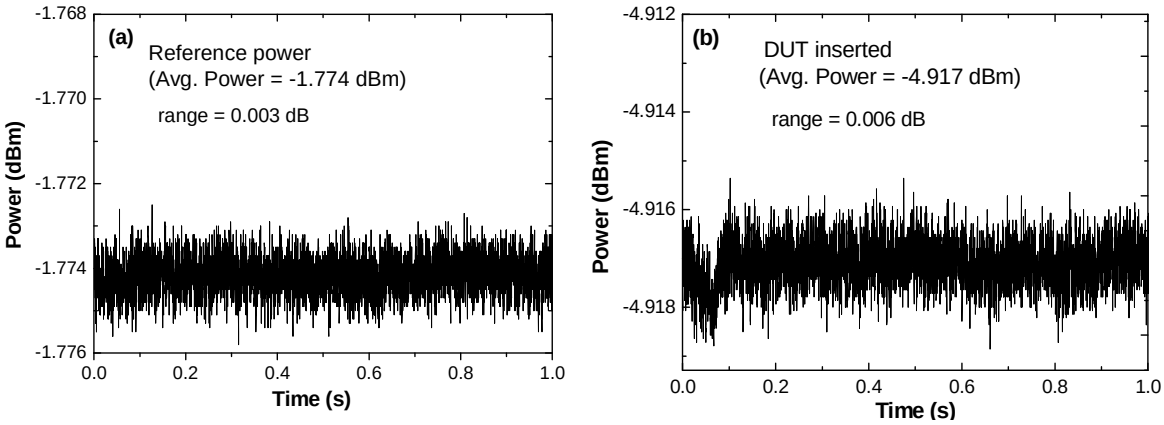

Figure 2.2: (a) Reference power measured without the 50:50 1×2 splitter and (b) transmitted power measured with the 50:50 1×2 splitter inserted in the setup.

There are 5286 data points generated within a second. The loss of the reference fibre was of the order < 0.001 dB. The insertion loss for the 50:50 1×2 splitter is 3.153 dB; this compared very well with specifications provided by suppliers (3.138 dB). The source stability of the power was between 0.002-0.006 dB for both reference power and after the DUT was inserted. The measurement was obtained from an EXFO IQS 500 Intelligent Test System with IQS-1700 high-performance power meter and Fabry-Perot IQS-2100 light source at 1550 nm.

2.2. Optical Return Loss (ORL)

As the light signal is transmitted through the DUT, some of the light is scattered or reflected. The reflected light reaches the transmitter, degrades the laser performance and causes interferences within the transmitted signal. The system performance is then limited. Optical return loss (ORL), sometimes referred as return loss, is a measure of the light reflected by a component. It is defined by the international standard bodies such TIA/EIA-455-107 as the ratio of the light power that is reflected from the component to the power of the light that is incident on the component and is expressed as follows:

$$ORL = -10 \times \log\left(\frac{P_{reflected}}{P_{incident}}\right) \tag{2.2}$$

As shown in the equation above, return loss will always be a positive value since the incident power, $P_{incident}$, will always be higher than the reflected power, $P_{reflected}$.

A higher return loss value means less reflected power and, thus, better performance. Return loss values for splitters, circulators and isolators in theory are expected to be greater than 50 dB.

To determine the return loss of an optical component the following measurements are performed:

1) The incident power $P_{incident}$ is measured by connecting the optical source directly to the power meter.
2) The reflected power $P_{reflected}$, is measured by connecting the optical source to the power meter via the DUT (see Figure 2.3).

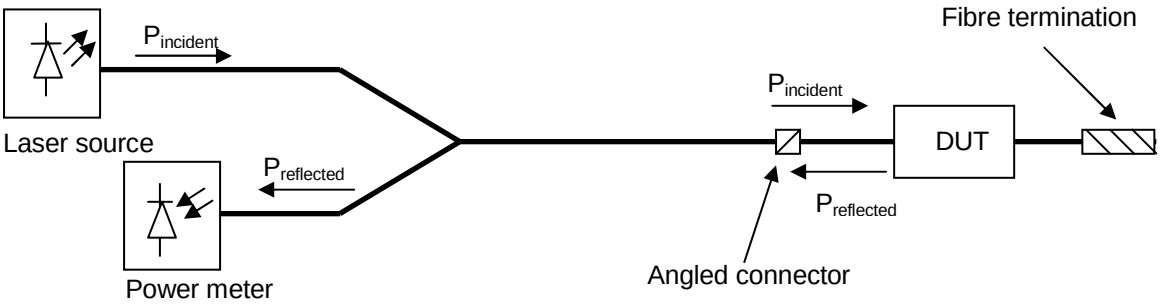

Figure 2.3: Illustration of experimental setup for the measurement of the ORL of optical components.

The end of the fibre is terminated to eliminate any unwanted reflections from the fibre cable or patchcord. This is achieved by bending the fibre in several tight fibre loops. The measured value is stored as a reference and the fibre is straightened and the ORL of the DUT is automatically calculated. Figure 2.4 shows the return loss measurement of a splitter and an isolator measured at a sampling rate of 1 Hz at 1550 nm with a total of 100 ORL values.

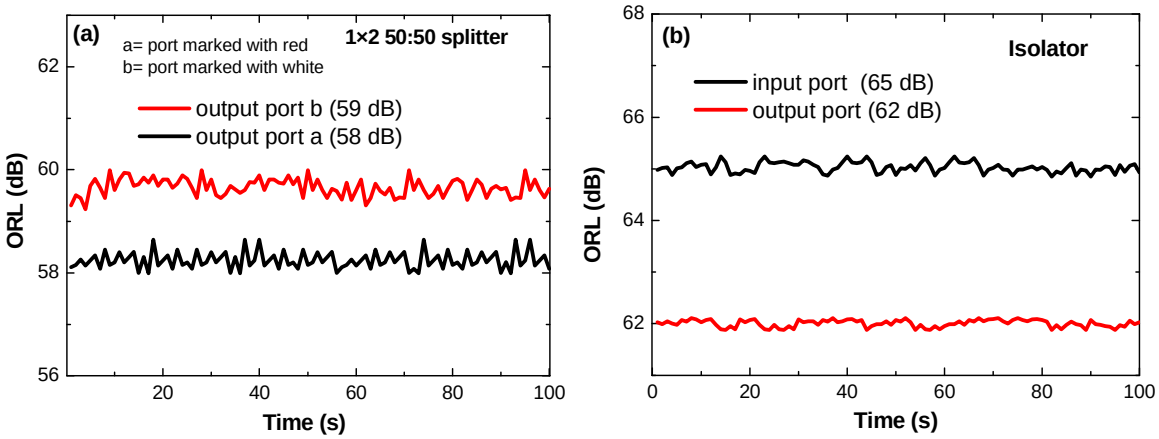

Figure 2.4: Return loss measurement obtained from the input and output ports of (a) a splitter and (b) an isolator.

The measurements of the return loss for an isolator and a splitter were obtained using EXFO's IQS-3200 return loss meter. The two output ports from a splitter gave a return loss of 58 and 59 dB respectively. Similarly the measured return loss from the input and output ports of the isolator were 65 and 62 dB respectively.

2.3. Polarization dependent loss (PDL)

Polarization dependent loss (PDL) is a measure of peak-to-peak difference in the optical power transmitted by an optical component or system for all possible states of polarization (SOPs) (Application note[2]). In contrast to an insertion or return loss measurement, a PDL measurement requires a polarization scrambler to scan all possible states of polarization (SOPs) of the DUT. The PDL of an optical component is then determined from the maximum and minimum difference in the output optical power. In contrast to other loss measurements, the polarization scanning method does not require a reference measurement. Measurement principle just relies on determining the difference of the maximum and minimum transmitted power, regardless of the incident power. More details on PDL are discussed in Chapters 3 to 6.

The work of this dissertation focuses on PDL measurements of optical components containing the polarization mode dispersion (PMD). Gisin and Huttner (1997) and Gisin, Huttner and Cyr (2000) in most of their research showed that it is not sufficient to characterize PMD and PDL separately since in telecommunication

networks consisting of long lengths of fibre, PMD and PDL will always be present. Liang *et al*. (1999), Lu *et al*. (2001), Wang *et al*. (2003) and other researchers together with results given in this dissertation, highlight the importance of considering both PMD and PDL in optical fibre telecommunication networks. It will be shown to be important to consider both PMD and PDL in a transmission link, since their combined impairments can be quantified and appropriate measures taken to compensate for these effects.

CHAPTER 3

Polarization effects in optical fibres and components

Polarization dependent loss (PDL) and polarization mode dispersion (PMD) are two important properties that are encountered when dealing with long single mode fibre links incorporating many optical components. Studies of PDL and PMD and their concatenation in laboratory and field work have been conducted by various groups recently. In this chapter, the two polarization properties, PDL and PMD, will be discussed. The factors causing these two polarization effects, their definitions and their combined effects will be discussed.

3.1. Polarization Concepts

A beam of light can be thought of as being composed of two orthogonal electric vector field components that may vary in amplitude and frequency. When these two components differ in phase or amplitude polarized light occurs. Polarization has been extensively studied in optical fibre and a variety of methods are available to either minimize or exploit the phenomenon.

There are a number of different methods of describing the polarization state of the electric field vectors. One of them is the *Stokes vector method* and is obtained by the following measurements

$$\vec{s} = \begin{bmatrix} s_0 \\ s_1 \\ s_2 \\ s_3 \end{bmatrix} = \begin{bmatrix} E_{0x} + E_{0y} \\ E_{0x} - E_{0y} \\ 2E_{0x}E_{0y}\cos\delta \\ 2E_{0x}E_{0y}\sin\delta \end{bmatrix} \tag{3.1}$$

where $\vec{s}$ is the Stokes vector with represented Stokes parameters ($s_0, s_1, s_2,$ and s_4). E_{0x} and E_{0y} are the amplitudes of the electric field components E_x and E_y. δ is the phase of electric components E_x and E_y. With this method it is possible to describe any arbitrary polarization state. The degree of polarization (DOP) is defined as

$$DOP = \frac{I_{polarized}}{I_{polarized} + I_{unpolarized}} \tag{3.2}$$

where $I_{polarized}$ and $I_{unpolarized}$ are the intensities of polarized and unpolarized light, respectively. When $DOP = 0$, light is said to be unpolarized and when $DOP = 1$, it is totally polarized. DOP is related to the Stokes vector by the following equation

$$DOP = \frac{\sqrt{S_1 + S_2 + S_3}}{S_0} \quad . \tag{3.3}$$

A point on the surface of the Poincaré sphere represented by the normalized Stokes parameters represents completely polarized light while a point within the sphere represents partially polarized light. In Jones representation, the polarized light is represented by a two-element complex vector given by:

$$\vec{E} = \frac{1}{\sqrt{E_{0x}{}^2 + E_{0y}{}^2}} \begin{bmatrix} E_{0x} e^{i\delta_x} \\ E_{0y} e^{i\delta_y} \end{bmatrix} \tag{3.4}$$

where δ_x and δ_y represent the phases of the electric field components E_x and E_y. If polarized light with Jones vector $\vec{E}_{in}$ is transmitted through a birefringent medium with no polarization dependent loss (PDL), the transmitted output Jones vector can be written as

$$\vec{E}_{out} = T(\omega)\vec{E}_{in} \quad . \tag{3.5}$$

The medium is represented by the transfer matrix $T(\omega)$, a function of a frequency dependent 2×2 complex matrix. It should be noted that the Jones representation is limited to the description of completely polarized light (Dericksson 1998, p.225)

The *Poincaré sphere* is another method of describing the polarization state and is closely related to the Stokes parameters. Any given polarization state corresponds to a unique point on the sphere. The centre of the sphere indicates unpolarized light. The north and south poles of the sphere represent right-hand and left-hand circularly polarized light, respectively. Points on the equator indicate various linear polarization states and all other points represent elliptical polarization states. Figure 3.1 represents the various polarization states within the Poincaré sphere.

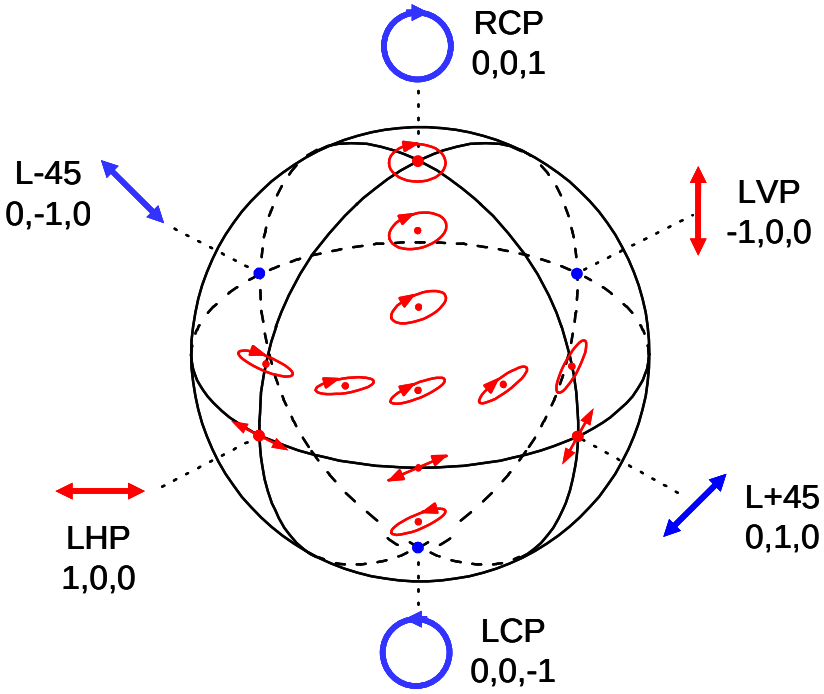

Figure 3.1: Poincaré sphere representing the various states of polarization (SOP) of polarized light signal.

There are several measurable polarization properties, inclusive of DOP, polarization dependent gain (PDG), polarization extinction ratio (PER), polarization dependent loss (PDL) and polarization mode dispersion (PMD). The following sections further outline the effects of PMD and PDL in optical networks.

3.2. Polarization mode dispersion (PMD)

Polarization mode dispersion was first investigated by Poole and Wagner in a paper entitled, “Phenomenological Approach to Polarization Dispersion in Long single-mode fibres” in 1986. Understanding the definition of PMD, its origin and effects on system performance, becomes important when planning to build a new optical network or when considering an existing link.

3.2.1. Definition and origin of PMD

An ideal single mode fibre supports one fundamental propagating mode which consists of two orthogonal polarization modes with identical group and phase velocities. These two orthogonal modes are called principal states of polarization (PSPs) to first order. In reality the PSPs are affected by the birefringence of the single mode fibre which leads to the difference in phase and group velocities of the polarization modes. The difference in the time of flight of the two polarization

modes through the fibre is called the differential group delay (DGD), represented by $\Delta\tau$ in Figure 3.2 (a). The letters f and s refer to the fast and slow PSPs, respectively. The magnitude of the birefringence and the orientation of the birefringent axes are not uniform in long length of single mode fibre, but vary randomly along its entire length. This results in an effect known as mode coupling and is represented in Figure 3.2 (b).

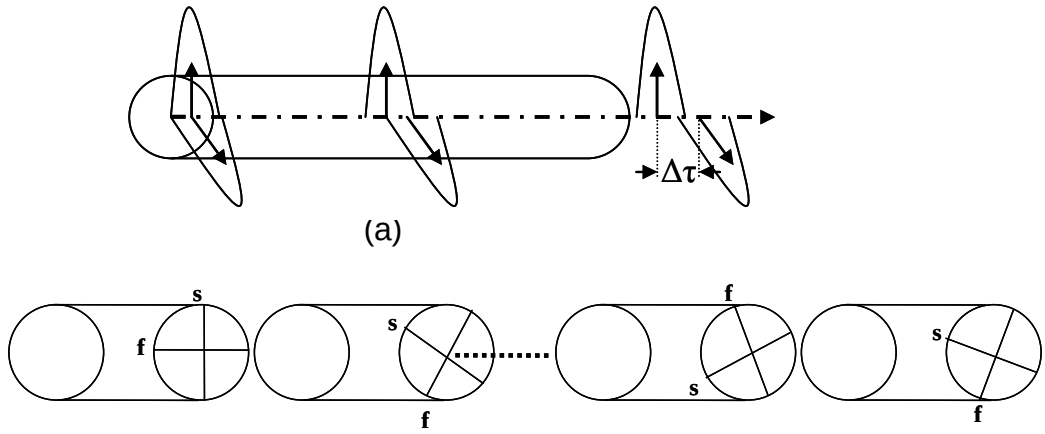

Figure 3.2: (a) The birefringence in single mode fibre causes dispersion of an optical pulse (b) variation in the birefringence of a long length of a single mode fibre.

The energy is coupled from the polarization modes of the first birefringent section to the polarization modes of the second section. “Any twist, bend or other external factor affecting the birefringence of an optical fibre will result in energy exchange between the two modes”, (Suetsugu *et al.* 1995). Hence stresses, bends and defects lead not only to birefringence, but also to mode coupling. The mode coupling and energy sharing result in a random variation with optical frequency, of the overall polarization modes, the PSPs and the DGD of the concatenation. The combined effects of birefringence and mode coupling lead to polarization mode dispersion (PMD).

There are many mechanisms that cause birefringence in optical fibre. The simple action of applying stress to, or bending a single mode fibre, induces birefringence. For example, Polarization maintaining fibre (PMF) has been manufactured through

specially introduced geometrical asymmetries. Figure 3.3 shows some of the causes of birefringence in single mode fibre.

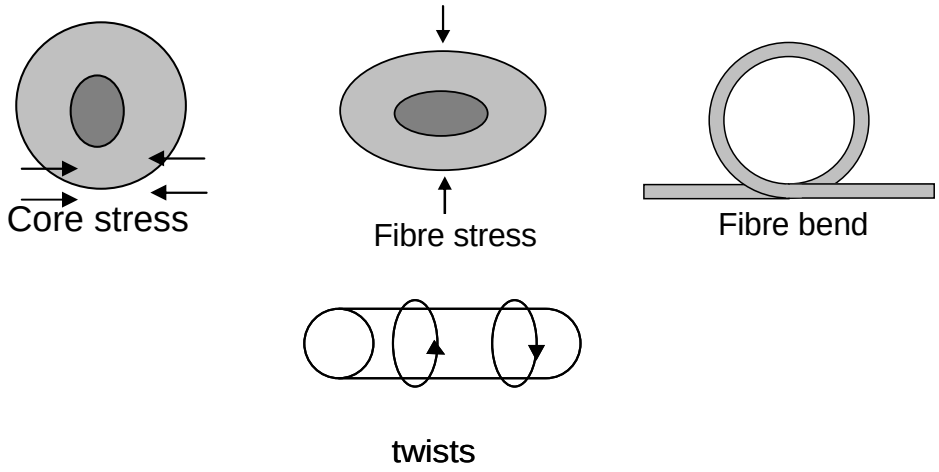

Figure 3.3: Factors causing birefringence in single mode fibre.

Traditionally, an investigation on PMD has mainly focused on optical fibre or systems as a whole, since PMD was considered to be negligible in optical components. More recently, the introduction of dense wavelength division multiplexing (DWDM) systems which incorporate many polarization sensitive components has lead to the measurement of PMD in optical components. It is very important to quantify the PMD of components as these devices present a way of increasing data rates using the existing infrastructure. Figure 3.4 shows some of the causes of PMD in optical components.

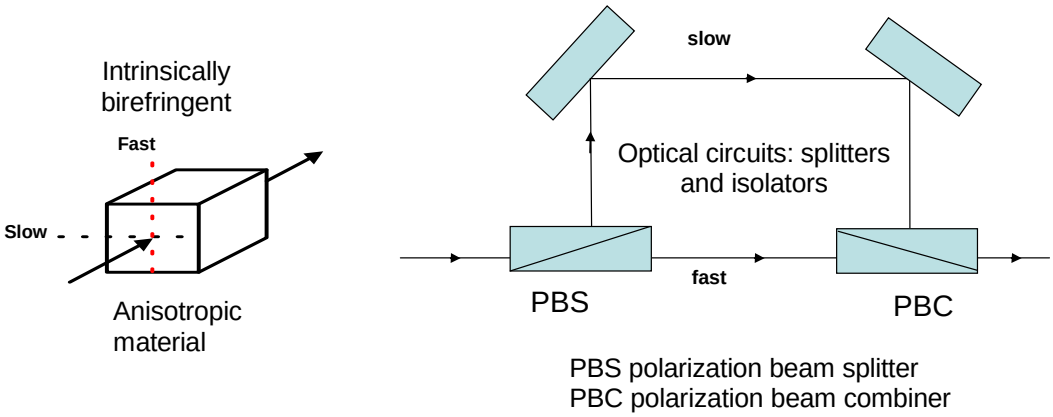

Figure 3.4: Some of the causes of birefringence in optical components.

3.2.2. Effects of PMD

According to Chou *et al*. (2001(2002), first order PMD depolarizes a scrambled polarized input so as to form an ellipsoid in Stokes space. Figure 3.5 is the experimental confirmation used to illustrate signal depolarization caused by PMD, obtained using the amplified spontaneous emission (ASE) source, a highly birefringent fibre and a polarimeter. The result was measured as part of this study.

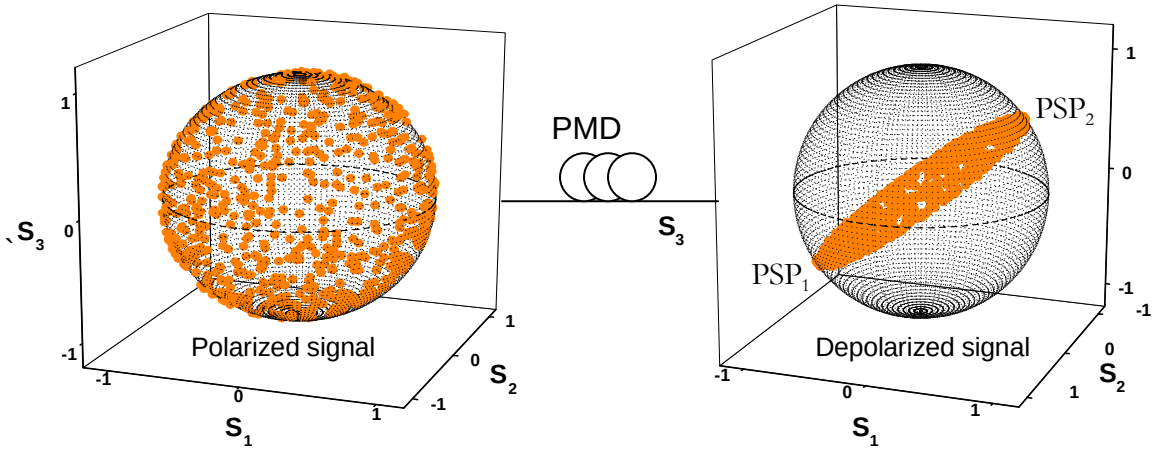

Figure 3.5: Depolarization of a signal caused by a link with polarization mode dispersion obtained using ASE source and a polarimeter.

The input state of polarization (SOP) is scrambled to cover the whole Poincaré sphere, as represented by Figure 3.5. The coverage of the Poincaré sphere should be relatively uniform and complete, so as to generate all possible SOPs. The PMD in the link depolarizes each of the scrambled input SOPs to a greater or lesser extent; this results in an ellipsoid being formed in Stokes space at the output of the fibre. Partially polarized light is represented by points within the Poincaré sphere as already mentioned in section 3.1. The nature of the ellipsoid provides information about both the principal states of polarization (PSPs) and the differential group delay (DGD) of the link being monitored (Gibbon 2007). Apart from depolarizing the polarized signal, PMD limits the transmitted signal by increasing the bit error rate (BER) (Boroditsky *et al*. 2004) and causes intersymbol interference (ISI) in digital systems and radio frequency (RF) power fading in analog or submarine-multiplexed transmission (Poole and Wagner 1986).

3.3. Polarization dependent loss (PDL)

One of the most critical requirements for characterizing dense wavelength division multiplexing (DWDM) passive components (filters, demuxes, muxes, gain flattening filters, OADMs, FBGs, attenuators, circulators, splitters/couplers, isolators and others) is the ability to measure PDL. The impact of PDL in passive components on optical network performance is increased power fluctuation which degrade optical signal to noise ratio (OSNR) and consequently higher bit error rate (BER) as already mentioned in Chapter 1. When combined with the polarization changes caused by mechanical stress, temperature or other environmental perturbations, PDL results in unwanted signal fluctuations. This deteriorates system performance and complicates power management. This section focuses on the definitions, origins and effects of PDL in optical transmission systems.

3.3.1. Definition and origin

Polarization dependent loss refers to the preferential energy loss of one of the PSPs (Gisin *et al*., 2000). It is the maximum peak to peak difference in transmitted power to all possible states of polarization (SOPs) as already defined in Chapter 2, section 2.3. International standard such as TIA/IEC-455-157 and IEC 61300-3-2 define PDL as

$$PDL = 10 \log_{10}\left(\frac{T_{\max}}{T_{\min}}\right) \tag{3.6}$$

where $T_{\max}$ and $T_{\min}$ are the maximum and minimum transmission intensities through the system. PDL is defined in decibels (dB) and is a positive quantity. Note that the following derivation of equation 3.6 was obtained following Damask (2005), pp. 300-302. The derivation is mainly done to show that the Jones space is equivalent to Stoke space. If one considers the Jones matrix of a PDL element aligned to the horizontal axis (S_1 in Stokes space), the output Jones matrix can be written as (Note that the angle between two Stokes vectors is double that of its corresponding Jones vectors):

$$\begin{pmatrix} v_1 \\ v_2 \end{pmatrix} = \begin{pmatrix} 1 & 0 \\ 0 & e^{-\alpha} \end{pmatrix} \begin{pmatrix} u_1 \\ u_2 \end{pmatrix} \tag{3.7}$$

where α is the loss coefficient. If the input intensity is represented as $\begin{pmatrix}1\\0\end{pmatrix}$, the output intensity is $|v_1|^2 = 1$. Similarly, for input intensity being $\begin{pmatrix}0\\1\end{pmatrix}$, the output intensity is $|v_2|^2 = \exp(-2\alpha)$. (Note that the Stokes space is a representation of light in three dimensional space related to the Poincaré sphere and the Jones space is a representation of light as a two-element complex vector and further discussion can be seen in section 3.1). The maximum transmission is 1 and minimum transmission is $\exp(-2\alpha)$. Since the ratio between the maximum and minimum transmission is $\exp(2\alpha)$ then the relationship between PDL equation 3.6 and the loss coefficient α related to Stoke space is

$$PDL = \alpha(20\log_{10} e). \tag{3.8}$$

Note that the 10 in equation 3.6 follows from the definition of dB. This relation holds true for any orientation of the PDL vector. The PDL vector is defined by $\vec{\alpha} = \alpha\hat{\alpha}$, where $\hat{\alpha}$ is a unit vector in Stokes space that points in the direction of maximum transmission. The transmission through a PDL element is given by

$$T_p = \frac{1}{1+\tanh\alpha}(1+\tanh\alpha(\hat{\alpha}\cdot\hat{s})). \tag{3.9}$$

The transmission depends on the loss coefficient α as well as the relative orientation of the PDL $\hat{\alpha}$ to the incoming state of polarization $\vec{s}$. Note that $\vec{s}$ is the state incident on the PDL element and is not necessarily the state launched into the fibre far away from the element. The transmission extrema (maximum and minimum transmissions) already mentioned are

$$T_p = \begin{cases} 1 & \hat{\alpha}\cdot\hat{s} = 1 \\ e^{-2\alpha} & \hat{\alpha}\cdot\hat{s} = -1 \end{cases}. \tag{3.10}$$

For a completely depolarized input, the transmission is averaged over all polarization states. It becomes clear that when $\langle\hat{\alpha}\cdot\hat{s}\rangle = 0$ then the average

transmission for unpolarized light is given by $\langle T_p \rangle = \frac{1}{1+\tanh\alpha}$, where $T_{depol} = \frac{1}{1+\tanh\alpha}$ is the transmission coefficient for depolarized light. From equation 3.9 the transmission through a PDL component becomes

$$T_p = T_{depol}\left(1+\Gamma\left(\hat{\alpha}\cdot\hat{s}\right)\right) \tag{3.11}$$

where $\Gamma = \tanh\alpha$ is the normalized loss coefficient. The transmission for depolarized light becomes;

$$T_{depol} = \frac{1}{1+\Gamma} \ . \tag{3.12}$$

Since $T_{\max} = T_{depol}(1+\Gamma)$ and $T_{\min} = T_{depol}(1-\Gamma)$, it follows from the above equations that the ratio between the maximum and minimum transmissions gives

$$\frac{T_{\max}}{T_{\min}} = \frac{1+\Gamma}{1-\Gamma} \ . \tag{3.13}$$

The identity $e^{2\alpha} = \frac{1+\tanh\alpha}{1-\tanh\alpha} = \frac{1+\Gamma}{1-\Gamma}$ and then PDL from equation 3.8 becomes

$$\rho_{dB} = \alpha\left(20\log_{10} e\right) = 10\log\frac{T_{\max}}{T_{\min}} . \tag{3.14}$$

Therefore equation 3.14 completes the derivation which shows that the Jones space is equivalent to the Stoke space.

PDL is caused by many mechanisms along a fibre optic link (TSB 141): Micro-optic components generate PDL due to the difference in the attenuated polarization modes of the transmitted signal. The passband frequency locations of integrated optic filters are polarization dependent, therefore they generate PDL. Splitters/fused couplers generate PDL due to polarization dependent coupling ratios. Micro-bends and macro-bends in fibres generate PDL. The material itself can generate PDL because of dichroism of the molecules, such as in polymer waveguides. Figure 3.6 illustrates some of the causes of PDL.

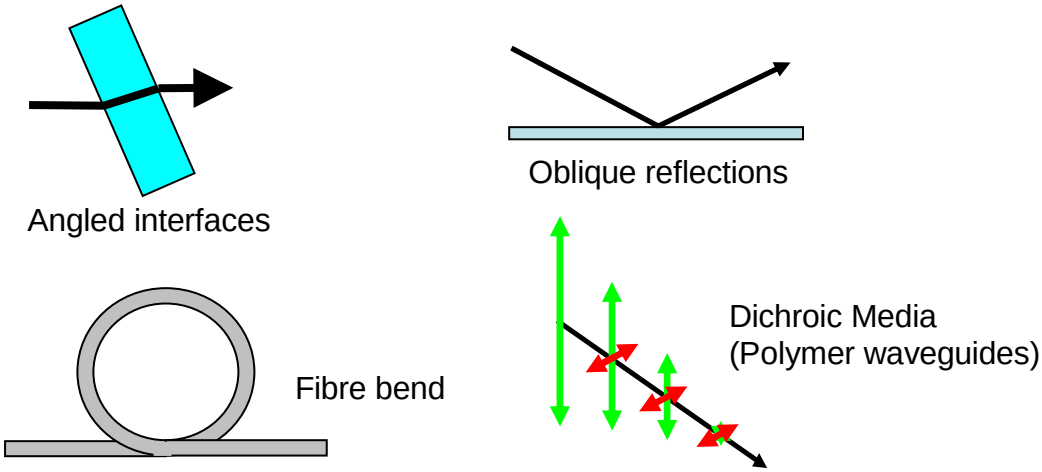

Figure 3.6: Some factors known to cause polarization dependent loss in optical fibre and components.

3.3.2. Effects of PDL

Components with high PDL values tend to polarize a partially or totally unpolarized signal. Figure 3.7 (a) shows an unpolarized signal that is polarized by a pure PDL component. A perfect polarizer transmits only states that have a finite projection along the polarizer axis. Figure 3.7 (b) shows how a circularly polarized signal's intensity is reduced when propagating through a partial PDL component.

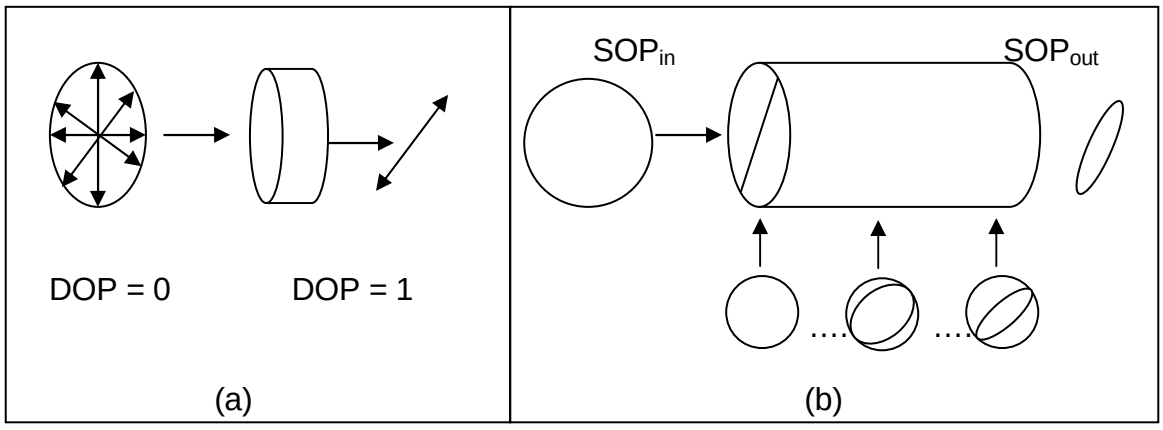

Figure 3.7: (a) depolarized signal is polarized after passing through a perfect polarizer; and (b) partial PDL element continuously changes the polarization state of the input light and reduces the overall intensity.

As the light travels the intensity is reduced along the loss axis of the PDL element while the intensity along the neutral axis is unchanged. It is evident how PDL transforms the polarization state along the component as the intensity gets reduced at various sites of the PDL component.

3.4. Combined effects of PMD and PDL

The concatenation of the birefringent elements and partial polarizers presenting PMD and PDL respectively, result in polarization effects that are more complicated than PDL or PMD alone.

The combined PMD and PDL results are summarised below:

1. The principal states of polarization (PSPs) are not orthogonal to one another when a link incorporates PMD and PDL (Gisin and Huttner 1997).
2. The output polarization state does not follow simple precessional motion as a function of frequency.
3. The PDL becomes wavelength dependent (Gisin and Huttner 1997).

Gisin and Huttner (1997) came up with many formulations to describe the combined effects of PMD and PDL.

3.4.1. Wavelength dependence of PDL

PDL is generally wavelength independent. However, the changing polarization states within sections of fibre exhibiting birefringence results in PDL being wavelength dependent. Therefore, the addition of some fibre exhibiting PMD to a system exhibiting PDL results in the PDL being wavelength dependent. The measurement of PMD-PDL, especially the characterization of its wavelength dependence for optical components, is critically important for system design and evaluation.

3.4.2. Non-orthogonality of principal states of polarization (PSPs)

In a system with PMD and PDL, Gisin and Huttner (1997) and Waddy *et al*. (2003) showed that the principal states of polarization vector can be represented by the following equation 3.15:

$$\vec{W}(\omega) = \vec{\Omega}(\omega) + i\vec{\Lambda}(\omega) \tag{3.15}$$

where $\vec{W}(\omega)$ is a frequency dependent complex PMD vector, while $\vec{\Omega}(\omega)$ and $i\vec{\Lambda}(\omega)$ are the real part and imaginary part of the PMD vector $\vec{W}(\omega)$. The imaginary term $i\vec{\Lambda}(\omega)$ occurs when PDL is present in the link. In the absence of PDL $\vec{\Lambda}$ is zero and $\vec{W}$ is real and its direction corresponds to the fast PSP. The presence of PDL results in $\vec{W}$ being complex and the fast PSP and slow PSP are not orthogonal anymore (Gisin and Huttner 1997). In reality PMD is always complex since PMD and PDL are always present even if one of PMD or PDL is very small (Waddy *et al.* 2003). The normalized output SOP described on the Poincaré sphere obeys the following equation of motion

$$\frac{d\vec{S}}{d\omega} = \vec{\Omega} \times \vec{S} - (\vec{\Lambda} \times \vec{S}) \times \vec{S} \tag{3.16}$$

where $\vec{S}$ is the normalized Stokes vector, ω is the angular frequency of the light, and $\vec{\Omega}$ and $\vec{\Lambda}$ as described above represent PMD and PDL. According to Poole and Wagner (1986) and Gisin and Huttner (1997), one can easily find out the output fast or slow Stokes vectors from the condition.

$$\frac{d\vec{S}_p}{d\omega} = 0 \tag{3.17}$$

where $\vec{S}_p$ is the fast or slow Stokes vector and ω is the frequency. By substituting equation 3.16 into 3.17 with $\vec{S}$ replaced by $\vec{S}_p$ one obtains the following:

$$(\vec{\Omega} - (\vec{\Lambda} \times \vec{S}_p)) \times \vec{S}_p = 0\,. \tag{3.18}$$

The left hand side of equation 3.18 consists of two vectors. Consider the definition of the cross product $\vec{A} \times \vec{B} = \left|\vec{A}\right|\left|\vec{B}\right| \sin\theta\, \hat{n}$, where θ is the angle between vectors $\vec{A}$ and $\vec{B}$ $(0 \le \theta \le 180^0)$ and $\hat{n}$ is the unit vector perpendicular to the plane containing $\vec{A}$ and $\vec{B}$. If $\vec{A} \times \vec{B} = 0$, θ is 0° or $180°$ which implies that either $\vec{A}$ and

$\vec{B}$ are parallel or anti-parallel. Therefore $(\vec{\Omega} - (\vec{\Lambda} \times \vec{S}_p))$ is parallel or antiparallel to $\vec{S}_p$ which implies that

$$\vec{\Omega} - \vec{\Lambda} \times \vec{S}_p = \lambda \vec{S}_p \tag{3.19}$$

where λ is a real eigenvalue to be determined with $\vec{S}_p$ being the generalized principal states of polarization (SOPs). According to Waddy *et al*. (2003), Chen *et al*. (2004) and Gisin and Huttner (1997), equation 3.19 can be solved to obtain the following solutions:

$$\vec{S}_p^{\pm} = \pm \left[\frac{\lambda}{\lambda^2 + \Lambda^2} \vec{\Omega} + \frac{\left(\vec{\Omega} \cdot \vec{\Lambda}\right)}{\lambda\left(\lambda^2 + \Lambda^2\right)} \vec{\Lambda} \right] + \frac{1}{\lambda^2 + \Lambda^2} \vec{\Omega} \times \vec{\Lambda}$$

$$\lambda = \sqrt{\frac{1}{2}\left[\Omega^2 - \Lambda^2 + \sqrt{\left(\Omega^2 - \Lambda^2\right)^2 + 4\left(\vec{\Omega} \cdot \vec{\Lambda}\right)^2} \right]} \tag{3.20}$$

The fast and slow outputs Stokes vectors $\vec{S}_p^{+}$ and $\vec{S}_p^{-}$ of the principal states of polarization in the above equation are not, in general, orthogonal to each other (unless $\vec{\Omega} \times \vec{\Lambda} = 0$, that is, $\vec{\Omega}$ and $\vec{\Lambda}$ are parallel or anti-parallel with each other which is very unlikely). The dot product of S_p^{+} and S_p^{-} is defined by the following equation

$$\cos\phi = s_p^{+} \cdot s_p^{-} \tag{3.21}$$

where ϕ is the relative angle between the fast and slow polarizations in Stokes space. From ϕ one can deduce the orthogonality of the PSPs. Note that ϕ is twice the real space angle in Stokes space. Figure 3.8 illustrates the non-orthogonality of the principal states of polarization.

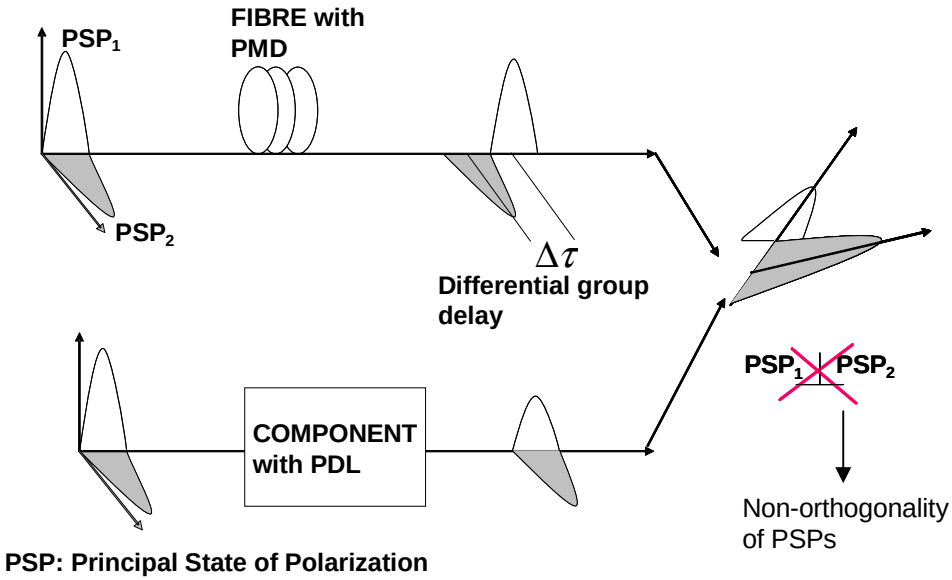

Figure 3.8: Illustration of the interaction between PMD and PDL. When PDL is present in a fibre link, the fibre PSP_1 and PSP_2 are no longer orthogonal.

Figure 3.8 shows that the input signal can be represented by two polarization modes, namely PSP_1 and PSP_2. By launching this signal in a fibre, polarization mode dispersion results in a time delay which is known as the differential group delay (DGD), $\Delta\tau$. When this signal is launched in a component with PDL, one of the PSP is attenuated more relative to the other. The combination of PMD and PDL results in these two PSPs being non-orthogonal.

3.4.3. Separation of PMD and PDL

Using polarization measurements, one can measure the Jones matrix of the concatenation between PDL and PMD, as first described by Gisin and Huttner, (1997). The matrix contains all the relevant information regarding the birefringence and the partial polarizers of the system. If one considers the general concatenation with random couplings, the transmission matrix becomes $T(\omega)$. According to Huttner *et al*. (2000), and Chen *et al.* (2005), there is a simple way to separate the effects of PMD and PDL. This follows from a theorem that any complex matrix, say T can be decomposed into the unitary matrix U and the Hermitian matrix A, which gives;

$$T(\omega) = A(\omega)U(\omega), \tag{3.22}$$

where U is the unitary matrix representing the effective PMD and A is the Hermitian matrix representing the effective PDL. From this decomposition, any concatenation with both PMD and PDL is equivalent to the concatenation of the purely birefringent element U, and the PDL element A. By multiplying T with its conjugate transpose T^{*t} we get $T^{*t}T = A^{*t}U^{*t}AU$ and since U is the unitary matrix ($U^{-1}U = I$) and $A^{*t} = A$ in case of the definition of the Hermitian matrix, the PDL of a component can be determined from

$$T^{*t}(\omega)T(\omega) = A^2 \geq 0 \tag{3.23}$$

where $T^{*t}(\omega)$ denotes the complex transpose conjugate matrix. According to Karlsson *et al*. (2000), A and A^{-1} can be obtained from A^2 and therefore we can obtain $U = A^{-1}T$. Finding the eigenvalues $T^{*t}(\omega)T(\omega)$ is equivalent to determining the PDL element A represented by equation 3.24:

$$PDL = 10\log\left(\frac{\lambda_2(T^{*t}T)}{\lambda_1(T^{*t}T)}\right) \tag{3.24}$$

where $\lambda_2 \geq \lambda_1$ are the eigenvalues. The eigenvectors of $T(\omega)T^{*t}(\omega)$ point in the direction of the cumulative PDL and the eigenvalues correspond to the maximum and minimum transmission through the PDL element. The PMD and PDL vectors are obtained by differentiating the Jones matrix (Gisin and Pellaux, 1992).

The complicated concatenation of several PDL elements intertwined between birefringent elements can thus be replaced by a much simpler system, with only one PMD element and one PDL element. Note also that A is not equal to all the concatenation of all the PDL elements, nor is U equal to the concatenation of the PMD elements (Huttner *et al*. (2000).

CHAPTER 4

Literature survey on PDL

Several research groups have studied PDL in optical components and optical fibres with and without PMD. The main objective of this chapter is to bring close attention to some of the findings on PDL by different research groups.

4.1. PDL in optical components

Passive optical components, for example isolators, circulators, splitters etc. are polarization sensitive and therefore exhibit PDL. When these components are concatenated each with some PDL the overall PDL is difficult to predict (Gisin *et al.* 1994). The concatenation of optical components containing PDL in optical telecommunication systems has been studied by many researchers, the findings of which are summarized below:

In the theoretical and experimental work of El Amari *et al*. (1998), two or more components each with PDL were concatenated and the mean, standard deviation and probability of the total PDL were presented. The total PDL was found to be less than the sum of each PDL element in the link. The reason has been attributed to the misalignment of the PDL axes at each connection, which tend to add or cancel the PDL in a section, thereby contributing to the global PDL in the link. Similar experimental results will be presented in Chapter 6, section 6.6.

In the theoretical work of Mecozzi and Shtaif (2002), the concatenation of a large number of PDL components was considered. They found that for linear concatenation of these components the global PDL grows as the square root of the number of components. On the other hand, in a recirculation loop, the global calculated PDL was found to grow linearly with the number of components (Vinegoni *et al*. 2004).

4.2. PDL in optical fibres

The PDL components interlinked with sections of single mode fibre containing birefringence result in wavelength dependent PDL. Knowledge of the wavelength dependent PDL is very important for system designers and manufacturers for the

management of power. The presence of PDL in optical fibres presents a challenge in PMD measurements due to their interesting interactions with PMD.

4.2.1. Wavelength dependent PDL

The concatenation of many PDL components combined with single mode fibres result in wavelength dependent PDL due to the relative orientation of the PDL axes. This is because each PDL component and birefringent segment in the concatenated link transforms the fixed input state of polarization (SOP) to a different output SOP, dependent on the wavelength due to its birefringent nature.

In the work of Yang *et al*. (2005) the total PDL was found to be wavelength dependent in the presence of fibre sections containing PMD. They considered the case of a pure PDL environment and found the PDL to be constant with wavelength while on the other hand a PMD object was inserted and they found PDL to change with wavelength.

4.2.2. Interaction of PDL and PMD

In systems with PDL and PMD the wavelength dependence of PDL as already mentioned above is observed. The reason is attributed to the orientation of the polarization states due to birefringence within sections of SM fibres, as previously discussed.

The theoretical work of Gisin and Huttner (1997) showed that a PDL element sandwiched between two fibres with PMD can increase the DGD of the link. They also found that in the presence of both PMD and PDL, the two principal states of polarization are not orthogonal; this leads to anomalous pulse width broadening.

In the experimental work of El Amari *et al*. (1998), two PDL components separated by an element presenting PMD were combined. They observed that for the case of two PDL components without PMD, the PDL is relatively constant with wavelength, while in the presence of PMD the PDL becomes wavelength dependent. The fluctuation of PDL with wavelength was observed to increase as the PMD value increases. Similar results are shown in Chapter 6 of this dissertation. In addition,

the PDL data can be used to infer the information on PMD. El Amari *et al*. (1998) showed that it is possible to extract the PMD information from PDL data based on the Fast Fourier Transform (FFT). For a known PMD value interlinked between PDL components, the value of PMD was determined by applying a Gaussian fit to the FFT data. Similar PMD results were obtained in this dissertation; section 6.7 shows good agreement of the PMD results obtained from the JME and FFT methods.

In the work of Lu *et al.* (2002), the outage probability induced by PDL and PMD was predicted using Monte Carlo simulations. The system consisted of 10 000 SM fibres with 100 PM fibre segments. They considered PDL values in the range of 0 to 0.04 dB and PMD values of 0 to 5 ps. They observed that the outage probability decreased as the power margin increased (0.3 to 1.0 dB) for links with PDL only, but they observed that this is not as effective for the case of combined PDL and PMD. Therefore, they concluded that an extra power margin is required for the case of PDL and PMD.

Gisin and Huttner (2000) simulated the bit error rate (BER) of a 600 km transmission link with 200 trunks with random mode couplings, each with 1 to 2 ps PMD. In addition, sections with 0.8 dB of PDL were added between each trunk with random orientations. They first plotted the BER with the influence of DGD only, and they added the PDL which resulted in an increase of the BER above the maximum value obtained with no PDL. Therefore the increase in the BER was attributed to the combined effects of PDL and PMD.

Sivasubramanian and Ravichandran (2007) in their theoretical work showed that pulse narrowing occurs in fibres when polarization dependent loss is present despite the presence of finite differential group delay leading to polarization mode dispersion. They observed that the pulse narrowing depended in addition on the state of polarization in which the input light was launched. They derived equations representing the optical power of the pulse for different cases of the input states of polarization in terms of PMD and PDL. They found from their equations that the pulse narrowing is prominent for a PMD of 30 ps, a PDL of 3.5 dB and an input

pulse width of 100 ps in different states of polarization for a PDL element sandwiched between two PMD elements.

4.3. PDL statistics

The probability density function of the polarization dependent loss (PDL) of a system with several components has been investigated by a number of groups (El Amari *et al*. 1998, Gisin and Huttner 2000, Mecozzi and Shtaif 2002, Vinegoni *et al*. 2004 etc.). However, there is a wide range of statements concerning the PDL statistics in the literature. El Amari *et al*. (1998) showed by derivation that when the number of PDL components is larger than two, the distribution is a Gaussian-like distribution. Mecozzi and Shtaif (2002) showed that the PDL is Maxwellian distributed when expressed in dB and is independent of the system's PMD which in this case the statistics will be due to the random signal polarization state between each component in the link. Lu *et al*. (2001) showed that PDL is Raleigh and Maxwellian distributed when considering pure PDL values and low DGD values.

In the work of Fukada (2002), a probability density function formula resulting from Jones matrix and Mueller matrix was used to predict the PDL in an optical system consisting of passive components and connecting fibres. The technique determines the transmission coefficients of the incorporated devices from their PDLs in a transmission system. They verified their analytical PDL results by a Monte Carlo numerical simulation where good agreement was observed.

Lu *et al*. (2001) performed simulations which showed that the probability density of PDL is a combination of Raleigh and Maxwellian distributions, for low DGD values of the order of 10^{-5} ps. When the DGD is 15 ps, they found that the PDL was Maxwellian distributed. In our PDL statistics we found that small PMD values of the order of 0.54 ps are approximated well by the Maxwellian distribution as opposed to high values 3 ps, which show a deviation from Maxwellian statistics. These results will be presented and discussed in section 6.7.

4.4. Compensation of PDL

High data rate optical fibre communication is one of the fastest growing areas in the telecommunication industry. The compensation of polarization effects is one of the major key technologies for high-speed and long haul data transmission. Much attention in the limitations of high-speed systems has been given to polarization mode dispersion. With the growth of WDM and DWDM technologies, various components incorporated in these technologies produce PDL which must be compensated for PDL.

Yan *et al*. (2002) in their experimental work use polarization scrambling at the beginning of the link and monitor down stream the power fluctuation induced by in-line components that exhibit polarization dependent loss (PDL). Their PDL compensation is accomplished by using the monitored PDL value as a control signal to vary a tuneable PDL module and minimize the power fluctuations. They perform PDL monitoring and compensation periodically along an 800 km link for four 10 Gb/s WDM signals. The PDL compensator reduces the 2 % power penalty distribution tail from 6.5 dB to less than 2 % in the presence of 14 ps average PMD.

CHAPTER 5

PMD AND PDL MEASUREMENT TECHNIQUES

This Chapter introduces the techniques used to measure polarization dependent loss and polarization mode dispersion. The particular methods used in this study are discussed in more detail.

5.1. PMD measurement techniques

PMD can be measured in either the frequency or time domain. In the frequency domain, the PMD manifests itself as a frequency dependent state of polarization, while in the time domain, the PMD is seen as time dispersion of the transmitted light pulse.

PMD in optical fibres and components can be measured using the following techniques, with some techniques more suitable under certain conditions than others, according to the IEC/CEI 60793-1-48 and CEI/IEC TR 61282-3.

Frequency domain techniques:
Jones matrix eigenanalysis technique (Heffner, 1992)
Fixed analyzer technique (Poole and Favin, 1994)
Poincaré Sphere Analysis (Galtarossa *et al*. 1996)
Attractor-Precessor Method (Eyal and Tur, 1997)

Time domain techniques:
Cross-correlation interferometric technique (Namihira, 1993)
Generalized interferometric technique (Cyr, 2004))
Phase shift modulation (Williams *et al*. 1999).

While four of these techniques are routinely used by the Optical Fibre Research Unit at the NMMU, in this study we focus only on the JME technique, since the same method can be used to determine PDL. From this method, PDL information can be used to extract the PMD information (Damask, 2005 and El Amari *et al*. 1998).

5.1.1. Jones matrix eigenanalysis (JME)

The transmission matrix of a monochromatic light wave through a linear medium such as optical fibre or a fibre optic component can be described in Jones vector formalism by $\vec{E}_{out} = T(\omega)\vec{E}_{in}$ as described in Chapter 3, where $T(\omega)$ is the frequency dependent transfer matrix that characterizes the medium. The measured matrix provides information on the differential group delay (DGD) and principal states of polarization (PSPs) of the device under test (DUT).

In order to determine the Jones matrix of an optical device, consider the three input states of polarization (SOPs) oriented at 0º, 45º and 90º. These SOPs generate a 2×2 matrix at each wavelength:

$$T(\omega) = \beta \begin{bmatrix} J_1 J_4 & J_2 \\ J_4 & 1 \end{bmatrix} \tag{5.1}$$

where β is a complex constant J_i are ratios obtained from the input and output Jones vectors of a specific input polarization. It can be shown (Heffner 1992, Heffner 1993 and Derickson 1998) that the DGD at the angular frequency midway between two closely spaced angular frequencies, ω_1 and ω_2, is given by:

$$\tau = \left| \frac{Arg\left(\rho_1 / \rho_2 \right)}{\omega_2 - \omega_1} \right| \tag{5.2}$$

where ρ_1 and ρ_2 are the eigenvalues of the matrix product $T(\omega_2)T^{-1}(\omega_1)$, and Arg denotes the argument function, that is $Arg\left(be^{i\rho}\right) = \rho$. Heffner (1992) showed that the fast and slow PSPs of the fibre are given by the two eigenvectors of $T(\omega_2)T^{-1}(\omega_1)$.

5.2. PDL measurement techniques

A number of techniques exist to measure polarization dependent loss (PDL) including: deterministic fixed states, pseudorandom all-states, unpolarized light and interferometric method (Zhou *et al*. 2007). The traditional deterministic fixed

states methods, namely the Jones Matrix Eigenanalysis (JME) and Mueller matrix method (MMM), employ a fixed number of input states of polarization (SOPs) to measure the PDL. The pseudorandom all-states method measures PDL from the difference in the output power as the input SOPs are varied to include all possible SOPs. Examples are the polarization scrambling method and the optical spectrum analyzer (OSA). Recently another fixed deterministic states method generating only two SOPs, called the *two states method*, has been reported by Zhou *et al*. (2007).

The JME, OSA and polarization scrambling methods will be implemented in this study for characterization of PDL measurements in optical components and fibres.

5.2.1. Polarization scrambling method

This is the easiest and most accurate method in comparison to the other methods for determining PDL since only one wavelength is specified for a PDL measurement of an optical component. In this method, polarized light is coupled into a time varying polarization controller (polarization scrambler), which is then coupled into the device under test (DUT). The light at the DUT output is measured by a high speed power meter. As the state of polarization (SOP) is rapidly varied by the polarization scrambler, the maximum and minimum output powers are recorded by the power meter. The PDL is calculated from the difference in the maximum and minimum powers or optical transmittance expressed in decibels (dB) using equation 3.6 in Chapter 3:

$$PDL = 10 \times \log\left(\frac{P_{\max}}{P_{\min}}\right) \tag{5.3}$$

where $P_{\max}$ and $P_{\min}$ are the maximum and minimum output powers, respectively (Derickson 1998).

The accuracy of the measurement is limited by the uniformity of the incident power level. It cannot be determined from the measured power values whether a change in power was caused by the DUT because of polarization dependent transmission properties, or because of a fluctuating output power at the source. Therefore a

high level of power stability is required. The power meter must be sufficiently fast (milliseconds scale) to capture all the extrema from the changing output SOPs.

Another complication in this method is the choice of the polarization scrambler. In order to make accurate measurements and sample all possible states, the polarization states that the scrambler produces need to be uniformly distributed on the Poincaré sphere. The appropriate polarization scrambling speed chosen is very important for the measurement of PDL. The scanning time also reduces the high uncertainties in the PDL results (this will be discussed further in Chapter 6 under the polarization scrambling method).

5.2.2. Optical Spectrum Analyzer (OSA)

Another method used to calculate PDL of a device based on determining the maximum and minimum powers is through using the optical spectrum analyzer (OSA). This is very similar to the polarization scrambling method. In this method the polarization state of the incident light is altered by manually varying the polarization controller. The variation in the output powers are used to determine the maximum and minimum powers and the difference is the PDL (in dB) of a device. The accuracy in this method is limited to the resolution bandwidth specified, the sweeping time which is affected by the sensitivity of the incorporated devices and the number of trace points selected relative to the chosen wavelength range. Therefore a suitable polarization scan time and appropriate trace points for the selected wavelength range will result in accurate PDL measurements.

5.2.3. Mueller matrix method

PDL of optical devices can also be measured by the Mueller matrix method (MMM). This method is based on generating four known polarization states to the device under test (DUT). The optical power transmission is then measured at these four states. The input signal, represented by its Stokes vector S_{in}, interacts with the optical device (DUT), represented by a four-by-four Mueller matrix M. The emerging light represented by its Stokes vector S_{out}, is defined as follows:

$$S_{out} = M \times S_{in} = \begin{bmatrix} m_{11} & m_{12} & m_{13} & m_{14} \\ m_{21} & m_{22} & m_{23} & m_{24} \\ m_{31} & m_{32} & m_{33} & m_{34} \\ m_{41} & m_{42} & m_{43} & m_{44} \end{bmatrix} \times \begin{bmatrix} S_0 \\ S_1 \\ S_2 \\ S_3 \end{bmatrix}_{in} . \qquad (5.4)$$

Indicating the total output power, the first element of S_{out}, is then given by

$$S_{out} = m_{11}S_{0in} + m_{12}S_{1in} + m_{13}S_{2in} + m_{14}S_{3in} \ . \qquad (5.5)$$

Only the matrix elements of the first row of the Mueller matrix, m_{11}, m_{12}, m_{13}, m_{14} are therefore needed to calculate PDL. For the four input SOPs at 0º, 90º, 45º and the right-hand circular state the transmission T can be obtained from the measured optical powers (Derickson, 1998) and is calculated as follows:

$$\begin{bmatrix} m_{11} \\ m_{12} \\ m_{13} \\ m_{14} \end{bmatrix} = \begin{bmatrix} \frac{1}{2}\left(\frac{P_A}{P_a} + \frac{P_B}{P_b}\right) \\ \frac{1}{2}\left(\frac{P_A}{P_a} - \frac{P_B}{P_b}\right) \\ \frac{P_C}{P_c} - m_{11} \\ \frac{P_D}{P_d} - m_{11} \end{bmatrix} = \begin{bmatrix} \frac{T_1 + T_2}{2} \\ \frac{T_1 - T_2}{2} \\ T_3 - m_{11} \\ T_4 - m_{11} \end{bmatrix} \qquad (5.6)$$

where $T_1 = \frac{P_A}{P_a}$ at 0º (linear horizontal polarization state),

$T_2 = \frac{P_B}{P_b}$ at 90º (linear vertical polarization state),

$T_3 = \frac{P_C}{P_c}$ at +45º (linear diagonal polarization state) and

$T_4 = \frac{P_D}{P_d}$, which is the right hand circular polarization state.

The capital subscripts (A, B, C, D) are measured powers at the four states with the DUT and the lower-case subscripts (a, b, c, d) are the measured powers without the DUT.

The maximum and minimum transmissions are expressed as follows (Derickson, p. 358, 1998);

$$T_{\max} = m_{11} + \sqrt{m_{12}{}^2 + m_{13}{}^2 + m_{14}{}^2}$$
$$T_{\min} = m_{11} - \sqrt{m_{12}{}^2 + m_{13}{}^2 + m_{14}{}^2} \quad . \tag{5.7}$$

PDL is then calculated using:

$$PDL = 10\log\frac{T_{\max}}{T_{\min}} . \tag{5.8}$$

Most optical components, inclusive of the polarization controller, have PDL. A reference measurement is therefore required prior to the insertion of the DUT, in order to take into consideration any residual PDL originating from measuring instruments and other components in the system.

5.2.4. Jones Matrix Eigenanalysis (JME) method

Compared to the Mueller matrix method which utilizes four SOPs to perform a PDL measurement, the JME method utilizes only three SOPs. From Chapter 3 the transmission properties of an optical device were represented by the complex Jones Matrix $T(\omega)$. The product of the Jones matrix and its conjugate transpose can be then be used to determine PDL of an optical component. Consider $T^{*t}(\omega)$ being the complex conjugate transpose matrix as in Chapter 3 (section 3.4.3), then PDL is determined from (equation 3.23):

$$T^{*t}(\omega)T(\omega) = A^2 \geq 0 \tag{5.9}$$

and finding the maximum and minimum intensity transmission coefficients is equivalent to finding the extrema values, that is, finding the highest and lowest values of $T^{*t}(\omega)T(\omega)$. Thus, $T_{\max}$ and $T_{\min}$ are given by the eigenvalues (λ_1, λ_2) of $T^{*t}(\omega)T(\omega)$ in equation 5.9 (Yang *et al*. 2005). Following from equation 3.24 in section 3.4.3 of Chapter 3, PDL is determined from:

$$PDL = 10\log\frac{T_{\max}}{T_{\min}} = 10\log\frac{\lambda_2(T^{*t}T)}{\lambda_1(T^{*t}T)} \tag{5.10}$$

5.3. Comparison of the three PDL measurement techniques

All the three methods have been used for characterizing PDL in optical components and optical fibres (Kim and Buerli, 2000). The main advantages of the polarization scrambling method are its simplicity, speed and accuracy. The optical spectrum analyzer method (OSA) is simple to use. It is only limited by the polarization states it produces through the DUT and is also time consuming. Any residual PDL of the measurement system, which in this case incorporates the polarization controller and power meter, will directly contribute to the uncertainty of the measurement.

The JME and Mueller matrix methods are not necessarily easy to use as they incorporate the use of matrices. The Mueller matrix method produces accurate results while the accuracy of the JME is limited by its high sensitivity due to the measurement of SOPs. The main disadvantage is their measurement complexity and the need for extreme care during measurement to avoid any external disturbances which might lead to errors in obtaining PDL results of a DUT. A comparison between the polarization scrambling, JME and OSA measurement results will be shown in Chapter 6. The Mueller matrix method is not considered since it has a similar operation principle to the JME technique.

5.4. Experimental setups

In this section the experimental setups used in this work to measure the PDL of optical devices and fibres using the JME, OSA and polarization scrambling techniques are shown.

5.4.1. Polarization scrambling method

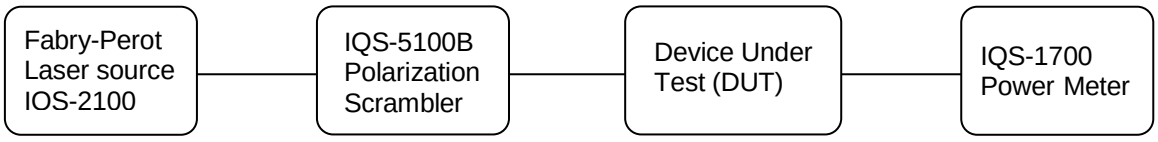

Figure 5.1: PDL measurement set-up using the polarization scrambling method.

The setup consists of a Fabry-Perot laser source (EXFO IQS-2100), polarization scrambler (EXFO IQS-5100B) and power meter (EXFO IQS-1700), which are all housed in the IQS-500 Intelligent Test System. The spectral range of the source is

between 1525nm to 1580 nm with resolution of 0.01 nm. Figure 5.2 shows the spectral range of the IQS-2100 Fabry-Perot laser source obtained using the optical spectrum analyzer. This measurement was done as part of this study.

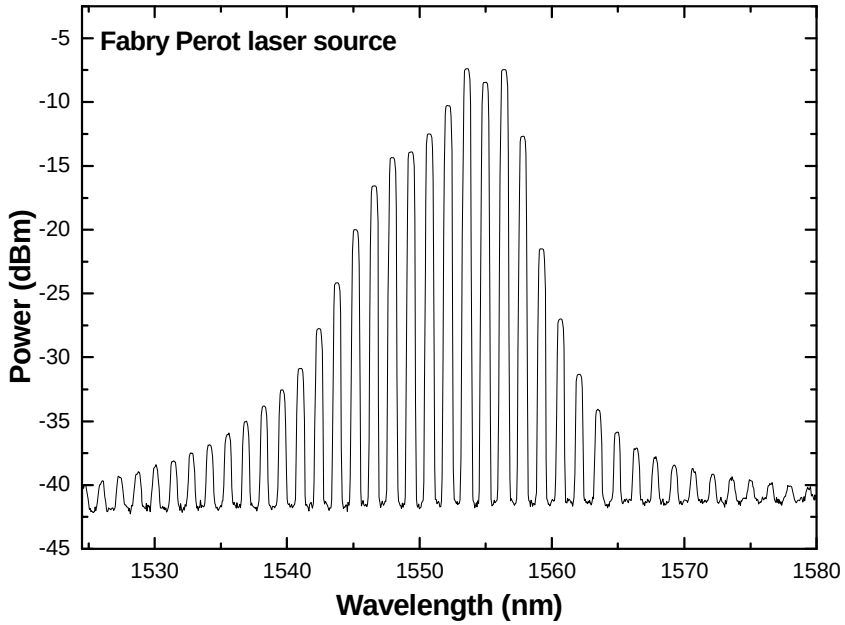

Figure 5.2: Spectrum of the IQS-2100 Fabry-Perot laser source obtained using the optical spectrum analyzer.

The scrambling speed can be varied from 0.5 s up to 99.9 s according the required average of measurements. The power meter has a resolution of ±0.001 dB, stabilization time of 0.3 ms. The measurement of PDL should be performed on all polarization states. The results are the variations in the optical power, from which the PDL information of an optical component is determined. All measurements were conducted at a wavelength of 1550 nm.

5.4.2. OSA method

Figure 5.3 shows the setup used to measure PDL of optical devices using the optical spectrum analyzer (OSA).

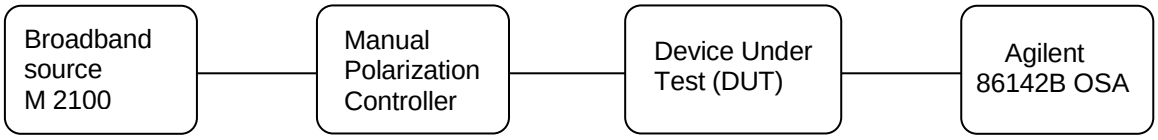

Figure 5.3: PDL Measurement set-up using the optical spectrum analyzer.

The polarized EXFO's M 2100 broadband source (1480-1620 nm), manual polarization controller (Lefebvre's loops) and the Agilent 86142B OSA power meter are used for measurement of PDL components using the OSA.

5.4.3. JME method

Figure 5.4 shows the experimental configuration for the PMD and PDL measurements using the JME method.

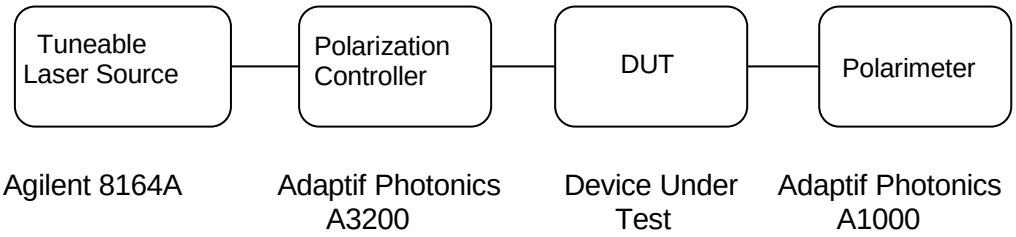

Figure 5.4: The experimental setup used to measure PMD and PDL using the JME method.

A tuneable laser source is used to scan over a specific wavelength range. At each wavelength, the transmission matrix of DUT is determined by measuring the output SOPs for three known input SOPs, namely 0º, 45º and 90º. Although any three distinct known input SOPs may be selected (Derickson 1998 p.225), the three linear SOPs (0º, 45º and 90º) are selected for simplicity of obtaining the transmission matrix of an optical device. It is very important to wait for about 10 minutes after setting up the experimental equipment to make sure the system is not vibrating. This is done to keep as low as possible the influence of the incorporated equipment other than the DUT, to reduce additional PDL that might lead to incorrect measurement of the PDL for the DUT. Measurements with the JME method require a stable environment for accurate results.

CHAPTER 6

RESULTS AND DISCUSSION

As described in the previous chapter, we have implemented the polarization scrambling method, the optical spectrum analyzer (OSA) method and the Jones matrix eigenanalysis (JME) method to measure the PDL of optical fibres and passive optical components. We start by analyzing PDL results from individual components obtained using the three methods separately. A comparison of the results from the three methods is then presented and discussed. PDL results on buried and aerial fibres will be investigated. Concatenation of components with PDL is shown and the combined effects of PDL and PMD are then investigated. Finally the effect of PDL and PMD on bit error rate (BER) is investigated using simulation software from Virtual Photonics Transmission Maker 7.5.

6.1 PDL measurements using the JME method

In this section the PDL measurement results of different optical components were obtained using the JME method. Some of the commonly used optical devices and components at high transmission rates include isolators, splitters, attenuators as well as optical fibres. Characterization of these devices is necessary in the design and management of optical fibre communication systems.

The tuneable laser source was swept between 1520-1570 nm with a resolution of 0.1 nm. Figure 6.1(a) and (b) illustrate PDL measurement results for a 50:50 1×2 splitter and a 3 dB attenuator. In optical systems an optical splitter is used to combine or split input light into several different paths while an attenuator is used to reduce the amplitude of the input signal without changing its waveform. It can be seen in Figure 6.1 that the PDL changes with wavelength. The change of PDL with wavelength is attributed to the intrinsic imperfections resulting in birefringence in a component. Thus the input states of polarization through any PDL element results in varying output SOPs and therefore resulting in power fluctuation. Note also that the influence of the connecting fibres must be taken into consideration since they might lead to the non-negligible imperfections.

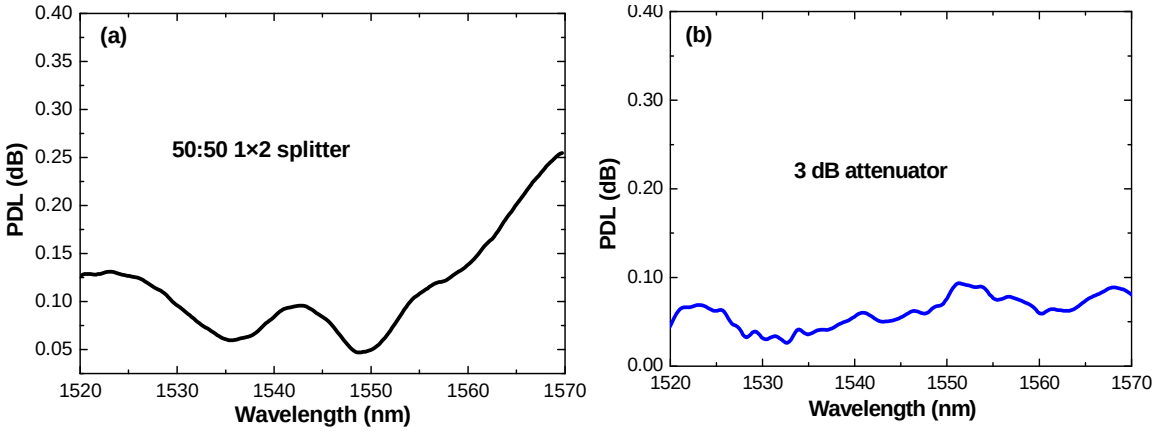

Figure 6.1: Spectral PDL measurement result for the (a) 1×2 splitter and (b) a 3 dB attenuator.

The wavelength range between 1550nm to 1570 nm shows a progressive increase of PDL with wavelength in Figure 6.1 (a). This is because the splitter has segments of single mode fibre (SMF) which are looped and this result in bend losses that tend to increase PDL for higher wavelengths due to macrobending. Harris and Ives (2002) and Lu *et al*. (2001) found that the presence of PMD of the order of 0.1 ps or less in the connecting fibres and also the birefringence within the components results in PDL being wavelength dependent. This is because a varying birefringence results from different magnitude of the connecting fibres and components which might result in mode coupling causing the observed PDL change with wavelength. Similar results have been obtained by Yang *et al*. (2005). They have reported that the PMD in optical components causes the PDL to be wavelength dependent. According to Yang *et al*. (2005) a large wavelength range is necessary to approximate the true status of the PDL component since each specific wavelength can be characterized for its own PDL value.

Figure 6.1 (a) is smoother than (b). The PDL fluctuations in Figure 6.1 (b) could be attributed to the high birefringence intrinsically present in the attenuator which makes it have strong wavelength dependence. Section 6.5, section 6.6 and section 6.7 present some wavelength dependence of PDL.

6.2. PDL measurements using the Polarization scrambling method

As already explained in Chapter 5, under the polarization scrambling method (section 5.2.1), the main principle relies on capturing the maximum and minimum

optical power over time as the polarization state of the light is continuously changed. The PDL is then taken as the difference between the maximum and minimum transmitted power. Accuracy in this method is limited by the scanning time selected and the power stability of the light source. The longer a polarization scan takes the smaller the uncertainty in the PDL values (Derickson, 1998) as more polarization states are generated through the device under test (DUT). Equation 6.1 shows the relationship between the PDL error (ΔPDL) and the measurement scan time for the polarization scrambling method:

$$\frac{\Delta PDL}{PDL} \alpha \frac{1}{scan\ time}. \tag{6.1}$$

The measurement system was left to stabilize for at least 20 minutes. The warming up of the measurement system is very important in order to ensure that the influence of the setup on the measured PDL results is kept to a minimum. Therefore a high level of power stability must be achieved for accurate PDL measurements.

In order to test experimentally the output uniformity, the input signal (EXFO Fabry-Perot laser source) was scrambled by using a EXFO IQS-5100B polarization scrambler and we then measured the corresponding output SOPs using an Adaptif Photonics polarization analyzer (A1000). The resulting Figure 6.2 shows the measured output SOPs at a sampling rate of 5 kHz and scanning period of 0.5 s.

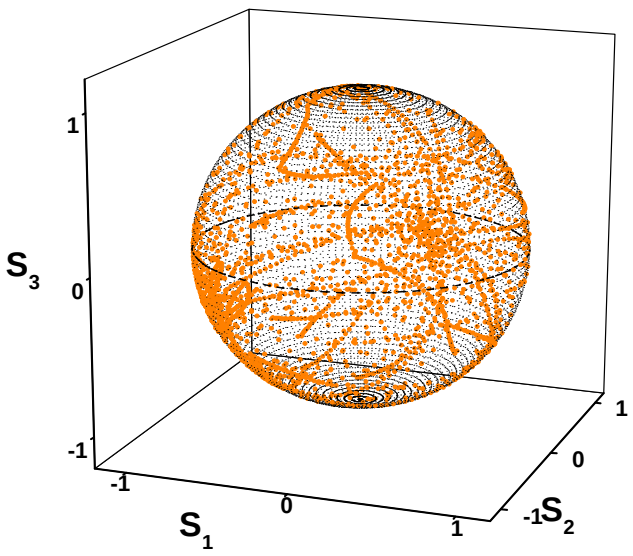

Figure 6.2: Representation of polarization states of the scrambled input signal measured for a period of 0.5 s and sampling rate of 5 kHz.

Moreover, it is necessary that the output states of polarization (SOPs) be uniformly distributed on the entire Poincaré sphere (Yang *et al*. 2005). As is evident in Figure 6.2, the output SOPs are uniformly distributed over the entire Poincaré sphere. This will result in accurate monitoring of polarization dependent loss as more output SOPs are generated and there is a better chance of finding the maximum and minimum powers relative to the number of output SOPs generated.

The accuracy of a PDL measurement will first be considered here: A series of PDL measurements were performed on an isolator by varying the scanning time. The PDL measurement *for each scan time* was repeated 20 times, during which the measurement setup remained undisturbed. By "undisturbed" in this case we mean obtaining the PDL measurement repeatedly, scan by scan without connecting or disconnecting the setup. The PDL error was then calculated from the standard deviation of the overall 20 scans. Figure 6.3 shows the PDL error as a function of different scan time selected. It can be seen that as the scan time increases the uncertainty in the PDL measurements is reduced. This can be explained by considering the fact that at longer times more SOPs are sampled, as already stated, so there is a better possibility of measuring the maximum and minimum powers.

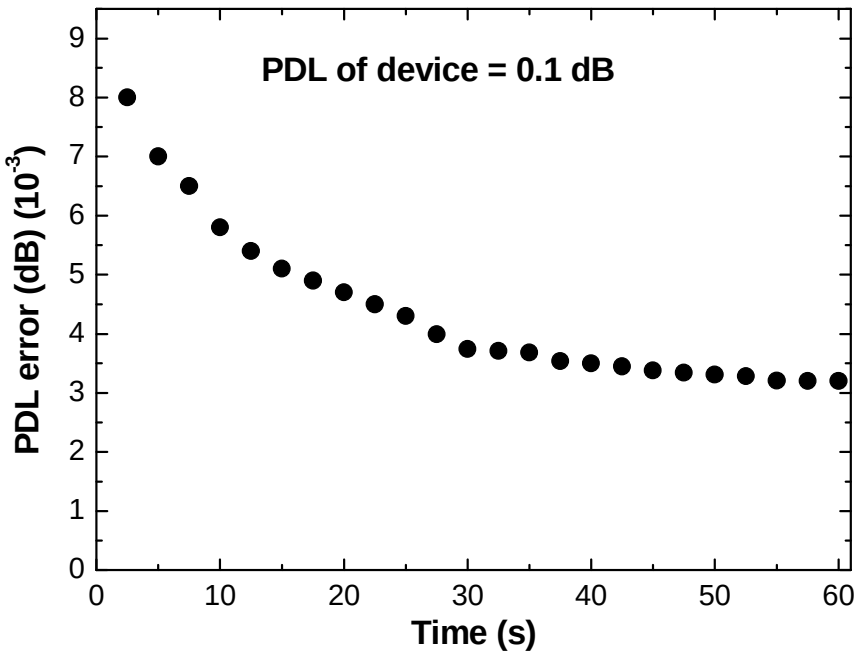

Figure 6.3: Calculated PDL uncertainty vs. the measurement scan time for the polarization scrambling method. Note that each scan time was repeated 20 times

When performing PDL measurements using the polarization scrambling method, much attention should be given to the power meter's averaging time and the scan rate of the polarization scrambler. This is because short averaging times will imply that shorter measurement times are required. The PDL uncertainty therefore is high since the numbers of polarization states generated by the polarization scrambler are small with short measurements times. A faster polarization scan rate implies more polarization states and therefore less PDL uncertainties. Longer averaging times on the other hand can result in incorrect PDL measurements since the maximum and minimum powers will be averaged out.

Figure 6.4 (a) and (b) shows the measured PDL results for the isolator and a shipping drum cable (6.03 km), as the input state of polarization (SOP) is varied for a scan time of 10 s. (An Optical isolator is used in fibre optic systems to propagate the signal in one direction while preventing the propagation of signals along a reverse direction that might interfere with the transmitted signal). The output power variation, where one finds the maximum and minimum powers, is used to determine PDL.

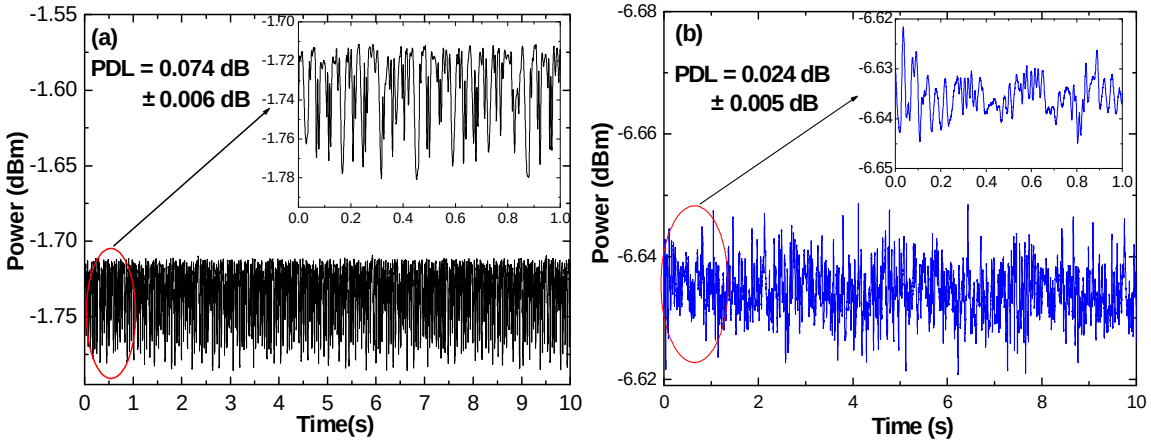

Figure 6.4: The power variation for (a) an isolator and (b) single mode cabled fibre on a shipping drum obtained using the polarization scrambling method with scan time of 10 s at 1550 nm.

It can be seen in Figure 6.4 (a) that the measured output power for the isolator is relatively uniform since there is uniform birefringence with little or no mode coupling. The shipping drum of undeployed cabled fibre on the other hand showed rapid power fluctuations. This could be attributed to the birefringence and mode

coupling within the fibre (of length 6.03 km). A PDL value of 0.074 ± 0.006 dB is obtained for an isolator, whereas the single mode fibre shipping drum cable consisting of 24 fibres, each 6.03 km in length, gave 0.024 ± 0.005 dB as shown in Figure 6.4 (a) and (b) respectively. Similar measurements of PDL for the same isolator were undertaken, this time the scan rate was selected at 60 s and Figure 6.5 shows the corresponding PDL results. It can be seen from Figure 6.5 that the obtained PDL value is 0.074 ± 0.003 dB. In this case the PDL value obtained for 60 s (0.074 dB) is similar to the one obtained for 10 s (0.074 dB). The only

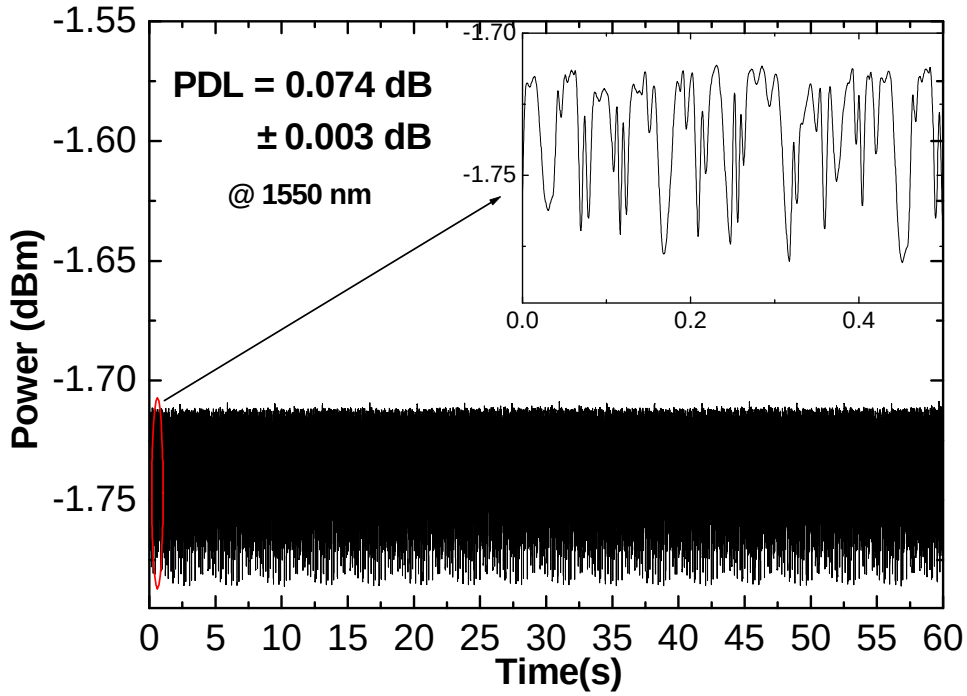

Figure 6.5: PDL measurement of an isolator, obtained using polarization scrambling method with a scan time of 60 s at 1550 nm.

difference is in the PDL uncertainty with 0.006 dB for 10 s and 0.003 dB for 60 s. It can be seen that increasing the scan time reduces the PDL measurement uncertainties as shown by Figure 6.5. Note that both measurements of Figure 6.4 and 6.5 were taken at 1550 nm wavelength.

6.3. PDL measurements obtained using the OSA

The OSA method is similar to the polarization scrambling method. The difference is only the polarization controllers, manual for OSA method and automatic for the polarization scrambling method. The drawback of this technique is high wavelength sensitivity and the insufficient generation of the polarization states.

Obtaining the maximum and minimum output powers in this method is not easy and so careful consideration must be taken into account when dealing with PDL measurements using the OSA. Another drawback is that this method is time consuming.

Figure 6.6 shows PDL measurement results for a 50:50 1×2 splitter (the same splitter as what was discussed in section 6.1). The number of data points collected was set to 10000 and averaging over 100 scans. Figure 6.6 (a) show the output maximum and minimum powers in dB as a function of wavelength while Figure 6.6 (b) plots the difference in the maximum and minimum output powers of Figure 6.6 (a), that is, the PDL, as a function of wavelength.

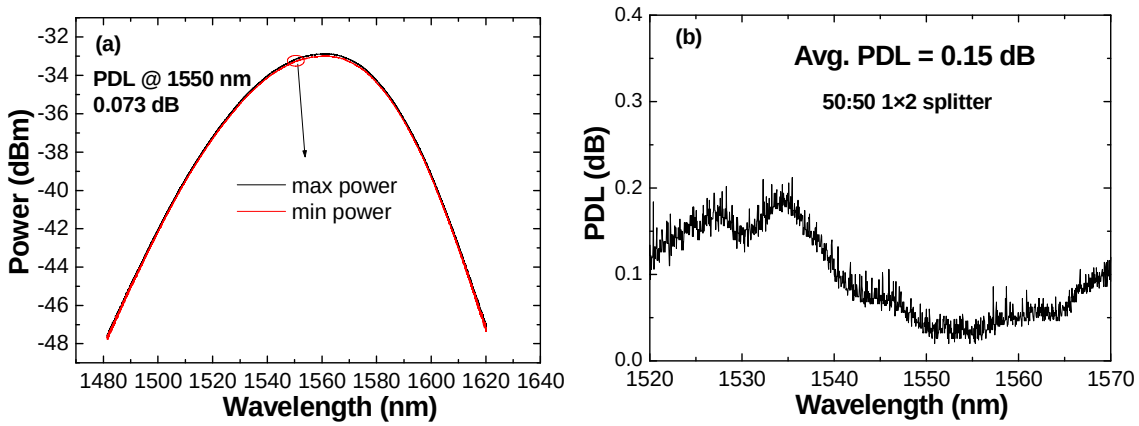

Figure 6.6: PDL measurement using OSA of a 50:50 1×2 splitter showing (a) max./min power spectrum and (b) calculated PDL spectrum (PDL=max.-min).

A PDL measurement of 0.073 ± 0.006 dB was obtained at 1550 nm as shown in Figure 6.6 (a). The spectrum was selected between 1520-1570 nm as shown by Figure 6.6 (b). The average PDL within the selected wavelength range was 0.15 ± 0.01 dB. As previously discussed, the PDL changes with wavelength could be attributed to the intrinsic imperfections resulting in birefringence in the component. The influence of connecting fibres (patchcords) contributes a negligible amount of PDL.

A dense wavelength division multiplexing (DWDM) multiplexer was also measured for PDL at 1550 nm as seen in Figure 6.7 (a). The result gave a PDL measurement of 0.035 ± 0.004 dB. Figure 6.7 (b) shows the spectral range

selected between 1549.0 nm to1551.5 nm. The standard deviations were obtained by performing 20 measurements, similar to the polarization scrambling method.

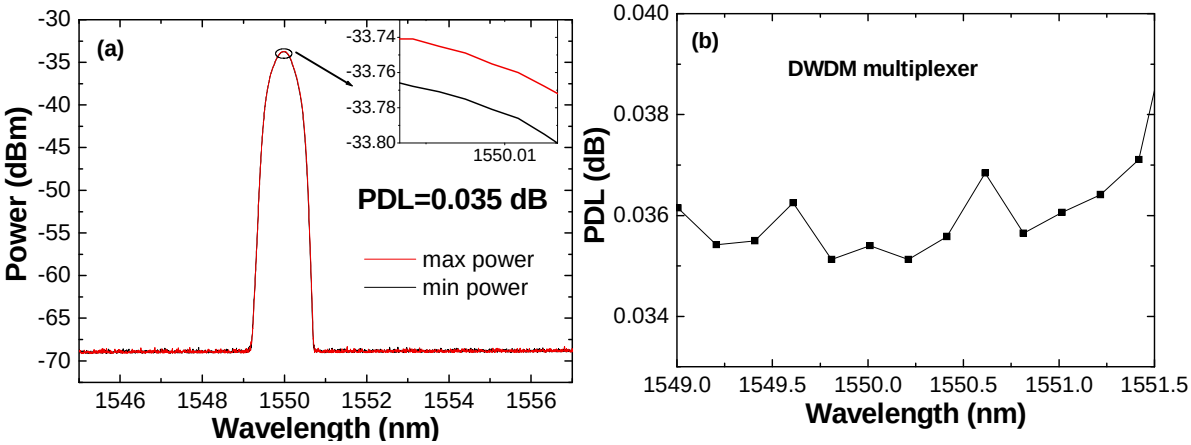

Figure 6.7: DWDM multiplexer (a) Power as a function of wavelength and (b) PDL as a Function of wavelength for the selected range.

6.4. Comparison of PDL measurements techniques

Measurements have been performed to compare the three techniques on a range of components. The PDL measurements were performed over a 1 minute period and at an interval of 2 minutes between each measurement. A set of 20 measurements were performed without disturbing the set-up and the results were compared at a wavelength of 1550 nm. This is the wavelength (1550 nm) at which the power meter in the polarization scrambling method is specified and also the measurement periods of 1 minute as already indicated in section 6.2 leads to lower uncertainty in the polarization scrambling method PDL measurements as shown in Figure 6.3. The results obtained are shown in Figure 6.8 for two of the devices, namely an isolator and a 50:50 1×2 splitter.

Figure 6.8 (a) and (b) show the PDL measurements respectively of the isolator and 50:50 1×2 splitter obtained using the three techniques: (polarization scrambling, JME and OSA). Both figures show a high fluctuation of JME results as compared to the polarization scrambling method and the optical spectrum analyzer. A possible reason for this could be attributed to the fact that in the JME method one measures the output states of polarization (SOPs) while in the polarization scrambling method and OSA one measures the output powers.

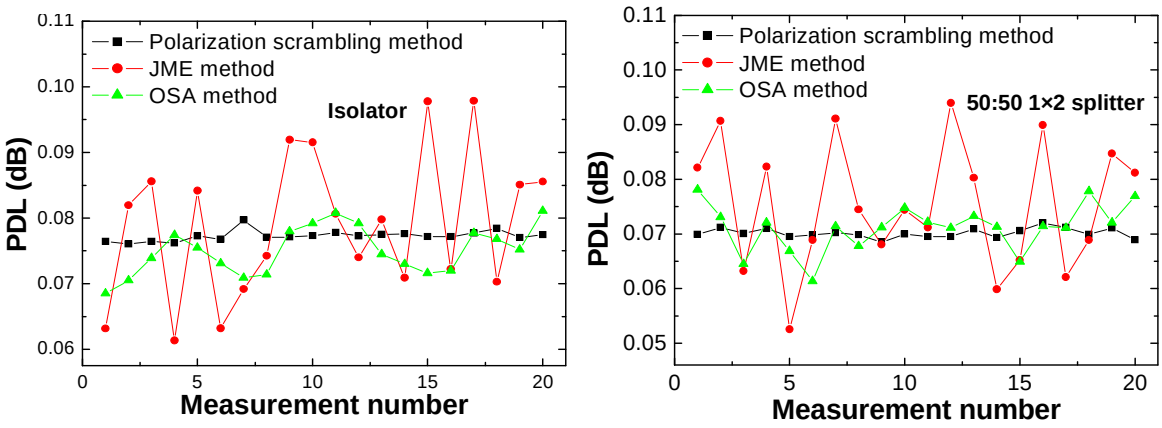

Figure 6.8: PDL measurement results for (a) isolator and (b) splitter obtained using the three techniques.

Also noticeable in Figure 6.8 is the relatively high PDL fluctuation of the OSA method in comparison to the polarization scrambling method. In the polarization scrambling method an automated scrambler is employed to randomize the input SOPs to different output SOPs which generate sufficient SOPs, while in the OSA method the input SOP is manually controlled and there is a high chance that not all possible SOPs are generated.

In order to make the comparison between the three methods more clearly, the mean values and standard deviations for the measured PDL values are listed in Table 6.1. The PDL results are generally in close agreement. The high standard deviations for the JME method are due to the large error as a result of the measured SOPs. The SOPs can be affected by the change of birefringence within connecting fibres and components while the power is less affected. This is in agreement with the experimental observation from Zhou *et al*. (2007). They showed that the SOPs can be affected by the change of birefringence within components during the measurement, while the power is less affected. Not only does the birefringence change the SOP, the topological (geometrical phase) effect can alter the SOP of the light signal. This results when the patchcord does not remain in one plane (for example suspended on the air upon which the fibre coil lies). Therefore the influence of the connecting fibres cannot be ignored.

Table 6.1: Comparison of PDL measurement results at 1550 nm obtained by the polarization scrambling, JME and the OSA techniques. Also included are product specifications as provided by the suppliers.

Components	Polarization Scrambling method(dB)	JME method (dB)	OSA method (dB)	Specification (dB)
Isolator	0.072±0.002	0.079±0.011	0.077±0.005	0.06
3dB Attenuator	0.051±0.003	0.055±0.008	0.053±0.004	0.05
Shipping drum	0.022±0.001	0.025±0.008	0.023±0.005	0.02
1×2 Splitter	0.070±0.003	0.075±0.010	0.071±0.005	0.07

6.5. PDL results of buried and aerial fibres

The field PDL measurements were obtained from fibres in a buried loose tube cable linking Sidwell and Linton Grange exchanges in Port Elizabeth. The length of the cable was 14.4 km which was looped to make an overall length of 28.8 km. The PDL measurements on aerial fibres were measured in St Albans (7.1 km aerial link extending from St Albans to Rocklands outside Port Elizabeth). The polarization scrambling method was used for the aerial and buried fibre measurements. The JME method was only used for buried links due to its high sensitivity to the environmental perturbations (wind, temperature and etc.) which makes it not suitable for the aerial PDL measurements. Since the OSA obtains PDL measurements in a similar manner to the polarization scrambling method, we were unable to use it in the field due to time constraints imposed by the network operator.

Figure 6.9 shows the power variation results for buried and aerial fibres obtained by the polarization scrambling method. There is a rapid power fluctuation for both the buried and aerial fibres. The measured PDL for both buried and aerial fibre is

0.080 ± 0.002 dB and 0.122 ± 0.010 dB respectively. It can be seen that the aerial fibre has high PDL uncertainty of 0.010 dB and this could be attributed to the environmental fluctuating effects such as temperature and wind that affect transmitted power.

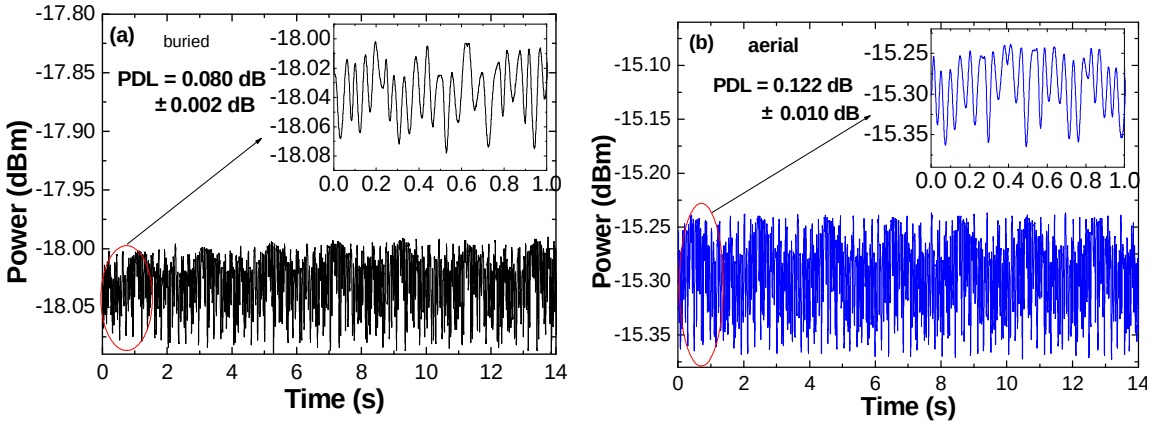

Figure 6.9: PDL measurements results of (a) buried fibre link and (b) aerial fibre conducted at 1550 nm wavelength.

The JME method was used to measure PDL for the same buried fibre link as above. Figure 6.10 shows the PDL versus wavelength spectrum. The PDL spectrum changes with wavelength due to the presence of PMD in the fibre. This is because sections of fibre present different magnitudes of birefringence which causes the change of polarization states with wavelength, therefore results in wavelength dependent PDL. Since the measured link was long (28.8 km) there are many mode coupling sites which makes PDL strongly wavelength dependent.

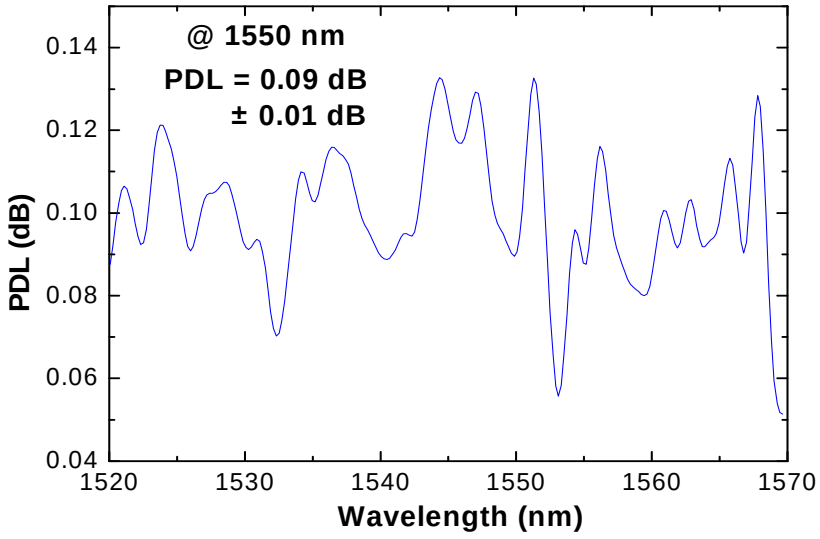

Figure 6.10: PDL versus wavelength measurement obtained using the JME method.

Polarization scrambling method and the Jones matrix eigenanalysis method gave 0.080 ± 0.002 and 0.090 ± 0.01 dB at 1550 nm for a buried link. The polarization scrambling method stands out to be a better method as compared to the JME and the OSA methods due to its accurate results and since it is the fastest of them all. Further illustration of wavelength dependence will be shown by some of the figures in section 6.7.

6.6. PDL results from the concatenation of the splitter

Having measured optical components separately in section 6.1 to 6.3, the concatenation of one of the components is investigated. Only the JME method is utilized in this section.

In figure 6.11 (a) a plot of PDL as a function of wavelength is shown for a concatenation of splitters. It can be seen that the addition of each splitter increases the global PDL in the link. The total PDL in the link is not simply the sum of the PDL values for individual splitters, rather, it is less than the expected total PDL value, (PDL_{AVG}). For example a single splitter (see Figure 6.11 (a)) had PDL_{AVG} of 0.11 ± 0.01 dB. By adding a similar splitter of the same magnitude we expected a value of 0.22 ± 0.02 dB but instead we obtained 0.18 ± 0.02 dB as evident in Figure 6.11 (a). This is due to the fact that the polarization sensitive axes of the PDL components are not aligned relative to each.

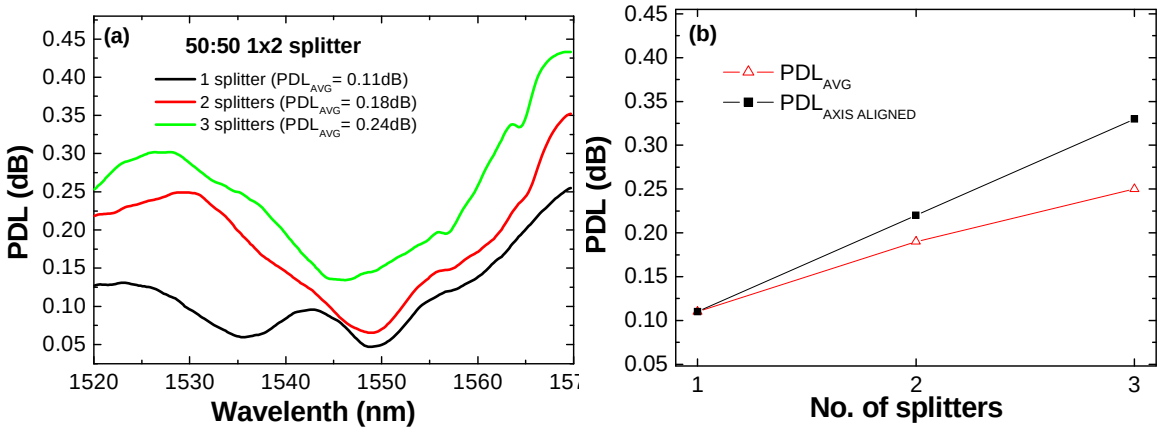

Figure 6.11: PDL variation as a function of (a) wavelength and (b) number of splitters for a concatenation of 1, 2 and 3 splitters.

Therefore the overall PDL depends on the relative random orientation of the PDL axes at each connection point. The PDL axis as defined by Gisin *et al*. (2000) is the point on the Poincaré sphere corresponding to the polarization state with minimum attenuation.

Figure 6.11 (b) shows the average PDL value obtained from the measured data of a single scan, and $PDL_{AXIS\ ALIGNED.}$ The latter is determined from the algebraic sum of the PDL of each individual component, assuming the PDL axes are aligned.

When designing an optical network, it is recommended to make use of individual components of approximately the same PDL magnitude (El Amari *et al*. 1998) in order to more accurately predict the global PDL. This is done to avoid the overall PDL being dominated only by the component with high PDL. A component with higher PDL than the others will lead to inaccurate prediction of PDL statistics and consequently inaccurate system power budget. Consider Figure 6.12, which shows the orientation of the PDL axis when they are aligned (left) and not aligned (right).

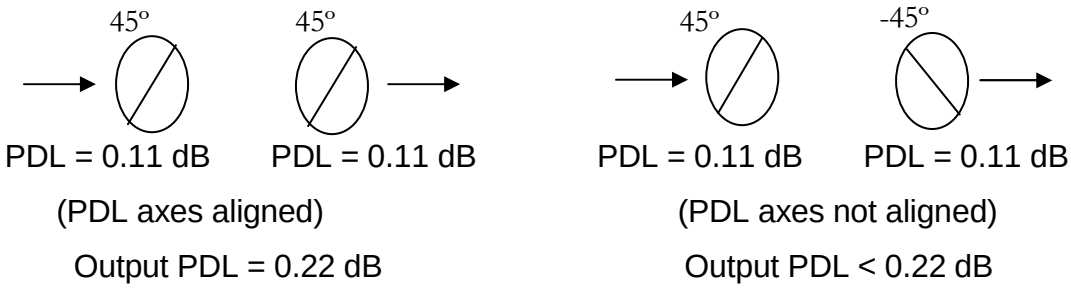

Figure 6.12: Representation of the transmission surfaces for aligned and nonaligned PDL axes/vectors.

The idea in the global PDL can be explained as follows: In the first case the PDL vectors are aligned, resulting in 0.22 dB overall PDL. However, in the second case the PDL vectors are misaligned resulting in the overall PDL being reduced due to the cancellation of the PDL vectors that tends to reduce the overall PDL. From figure 6.11 (b) there is a linear increase in the global PDL relative to the number of components when the PDL vectors are aligned. In a real system with concatenations of many optical components, the overall/system PDL can increase

or decrease depending on the relative orientation of the multiple PDL vectors of each component (Damask, 2005).

6.7. Interaction of PMD and PDL

This section investigates the interaction of PMD and PDL in further detail. The properties of PDL in the presence of PMD will be investigated-specifically, the influence of PMD on the statistics of PDL. All the results discussed in this section were obtained using the JME method.

6.7.1. PDL in PMD emulators

PMD emulators have been widely used in the investigation of PMD effects in optical transmission systems and also for the testing of compensating devices. They are a vital component in addressing the deleterious effects of PMD in optical telecommunication networks. Different PMD emulators have been developed using a series of PM fibres (Waddy *et al*. 2003, Dos Santos *et al*. 2002, Noé *et al*. 1999, Forno *et al*. 2000 and Hauer *et al*. 2002). The PM fibres are normally looped in diameters sufficiently large enough to avoid bending losses (dos Santos and von der Weid, 2004). Even if the bending loss is reduced, PDL is still generated due to the loss difference of the polarization modes. Therefore the bending introduced within sections of looped fibre generates PDL which results in distortion of transmitted signal caused by both PMD and PDL.

A PMD emulator was constructed as follows: A 10 metre PM fibre was equally divided and spliced into 8 segments with random mode coupled splice joints to generate a statistical PMD emulator. Each splice junction was considered a mode coupling site and each PM fibre segment was considered to contribute to overall PDL. The splice loss was kept to a minimum (≤0.02 dB) to avoid any unwanted losses that might influence the results by introducing errors. On the other hand, PDL was induced by making 5 turns of loops to the obtained PMD emulator so as to generate a PMD/PDL emulator. This is because for a fixed input SOP, bending introduced in the PM fibre induces additional birefringence which therefore changes the output SOPs, with certain states being attenuated more than other

states and thereby leading to extreme values of the output power and generating PDL.

6.7.1. (a) Bend-induced PDL

Figure 6.13 (a) and (b) respectively show the PDL spectra obtained for the PM fibre before and after being cut and spliced into 8 subsections to generate a statistical PMD/PDL emulator. The fast and slow polarization axes of the segments within the entire emulator are randomly aligned. Both figures show a PDL spectral change with wavelength. Higher PDL fluctuations with wavelength in Figure 6.13 (b) are attributed to the increased mode coupling sites which are introduced by the splice junctions (Kaminow, 1981).

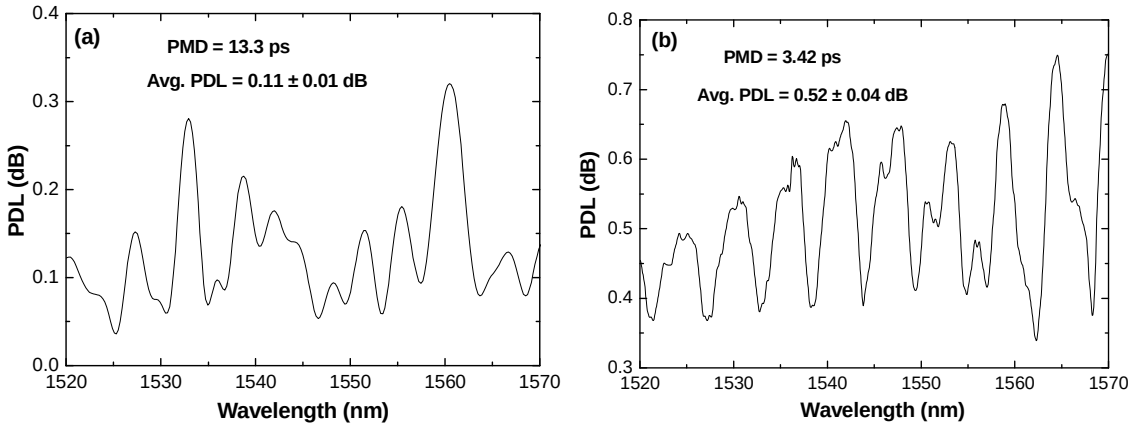

Figure 6.13: PDL signature obtained (a) from 10 m PMF and (b) after the PM fibre was Equally divided into 8 segments.

Initially, the average PDL and PMD before being spliced was 0.11 ± 0.01 dB and 13.3 ps as shown in Figure 6.13 (a). The error in the PDL value was calculated, similar to section 6.4, by determining the standard deviation of 20 scans of the PDL data. The increase of the average PDL after splicing is due to the individual segments that contribute to the overall PDL in the link. On the other hand, the PMD decreases and this is due to the induced mode coupling sites that tend to add or subtract PMD of each segment that contributes to the total PMD of the emulator. (This observation will be further explained in Figure 6.15 where all eight segments of the emulator are characterized). The progressive PDL spectral increase with wavelength (Figure 6.13 (b)) is attributed to the fact that at short

wavelengths the two polarization modes (fast and slow principal states of polarization (PSPs)) of the signal are well confined in the core region of the PM fibre (Hiirokazu *et al*. 2004). At long wavelengths the loss of the fast and slow axes begins to increase due to the added loss which results from macrobending (Keiser 2000, pp. 130-132). This trend was also observed by Zhou *et al*. (2007) and Dos Santos and Von Der Weid (2004).

Figure 6.14 shows the average PDL measured for one PM fibre section (10 metre PM fibre originally not spliced) as a function of different diameters. In this experiment, 5 turns of the PM fibre were generated around each diameter and the average PDL measured from the PDL signature. The insert is the measured PMD for the same diameters and turns.

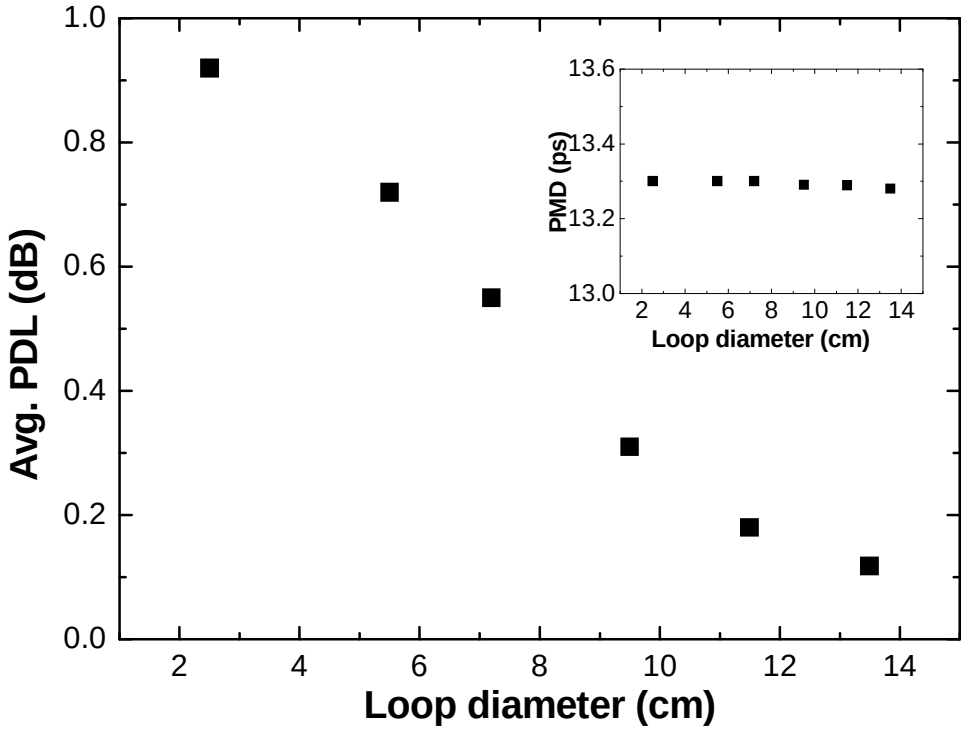

Figure 6.14: Average PDL as a function of the loop diameter (cm) for a segment of PM fibre (10 meter section). The insert is the PMD as a function of loop diameter.

These results indicate very clearly that the bending-induced PDL is high when the loop diameter is small. The PMD values, shown as insert, remain fairly constant with different diameters. From the results, we therefore conclude that the increase of PDL is due to losses associated with the bending introduced when generating

The author thanks Vitalis Musara for helping in the construction of the emulator

turns around the objects having a particular diameter (rather than losses associated with the mode coupling sites).

6.7.1. (b) Mode coupling

During the initial stages of the construction of the emulator all eight segments were characterized for PMD and PDL. Figure 6.15 shows the PMD and PDL results obtained from the eight segments. We observed that the PMD decreases as the number of sections increase. This is a result of the PMD vector cancellation enhanced by the randomly distributed mode coupling angles/sites. Mode coupling sites are intentionally introduced in single mode fibres and polarization maintaining fibres to lower the effects of PMD.

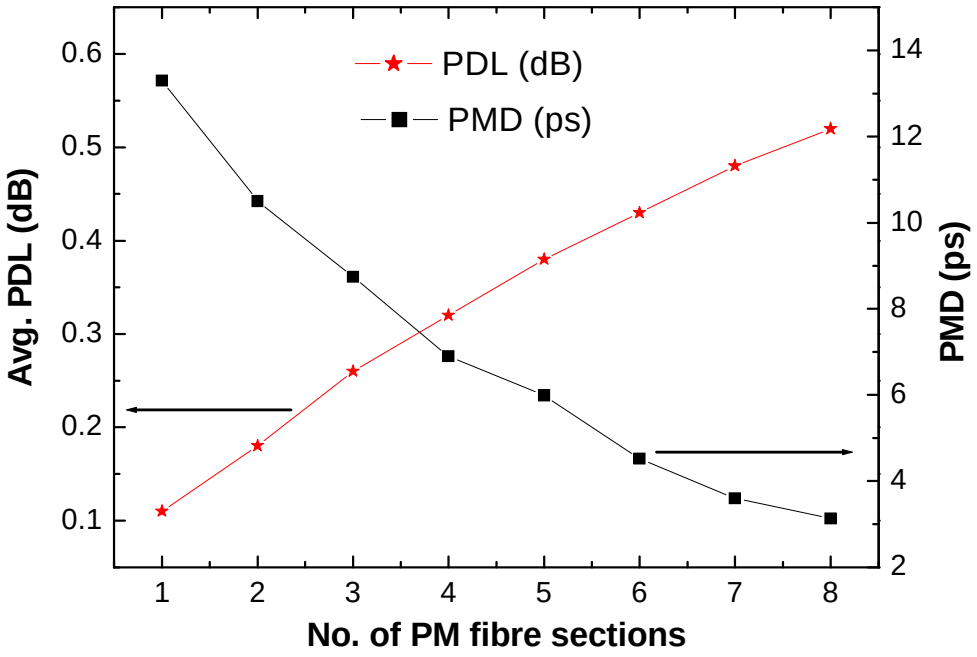

Figure 6.15: Variation of PDL and PMD with the number of PM fibre segments for 10 metre PM fibre

The average PDL increases as an increasing number of PM fibre segments are joined. This is because each segment contributes its own PDL and thereby leading to an increase in the overall PDL.

Since we have already mentioned that the PDL originates from each PM fibre segment and together contributes to the overall PDL in the link, according to El Amari *et al*. (1998) the total average PDL is not necessarily the sum of PDL

segments. Systems networks can be impaired with values even as small as 0.1 dB. For example, if one considers one section with an average PDL value of 0.11 ± 0.01 dB as indicated by Figure 6.15, the direct sum of eight segments results in 0.88 ± 0.08 dB but a value of 0.52 dB has been measured. The increase in PDL induces signal distortions and makes it difficult to compensate for PMD in real network systems.

6.7.2. Statistics of PDL in the presence of PMD

This section investigates the statistics of polarization dependent loss in the presence of low and high polarization mode dispersion. The effect of PMD on PDL statistics must be considered because a telecommunication link is considered as a concatenation of PMD and PDL elements. On the other hand, a long concatenation of pure PDL is unlikely in real telecommunication links.

Figure 6.16 shows the probability density functions (PDF) for the PDL of different numbers of concatenated components in the presence of three different values of PMD. It is obtained from the PDL spectra (shown as inserts) measured using the JME method. A bin size of 0.02 dB was selected.

Figure 6.16 (a) represents the PDF versus PDL for a concatenation of 5 components (3 splitters and 2 isolators) interconnected with single mode fibre sections. The average PDL for the concatenation is 0.19 dB. The bars represent the probability of certain PDL values occurring, while the solid line is the theoretical Maxwellian fit. The insert is the collected PDL spectrum from which the PDF is obtained.

Figure 6.16 (b) shows results for the concatenation of the five components as above and 3 added polarization maintaining fibres each of length 1.5 metres. The PM fibre each had a PMD value of 1.8 ps. The average PDL of the link was 0.32 dB. A deviation from the Maxwellian PDF is observed and this indicated by the areas not populated by the occurrence of PDL values. This could be attributed to

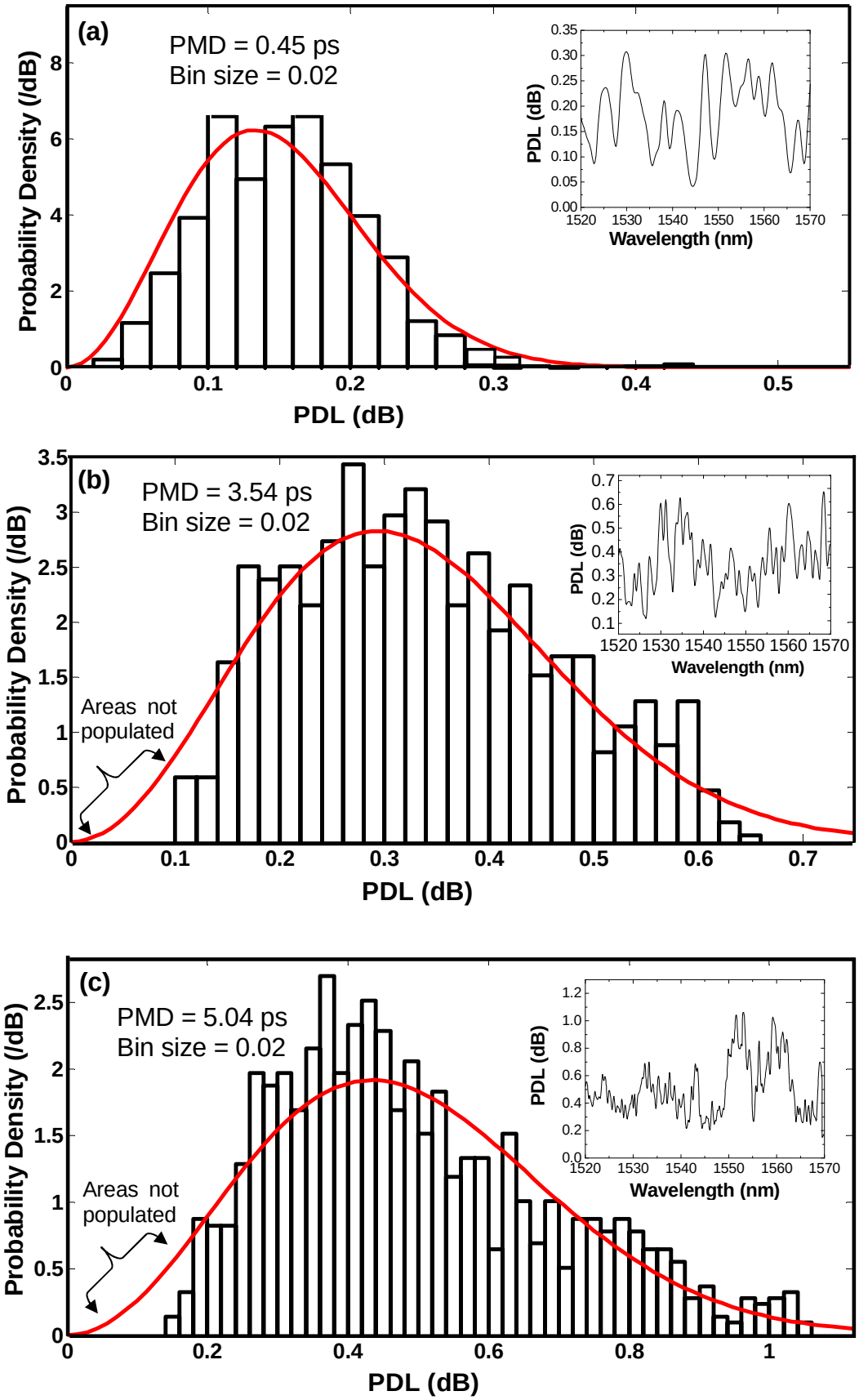

Figure 6.16: Probability density function versus PDL for different concatenated components (a) 5 components (b) 8 components and (c) 10 components.

the mutual interaction between PMD and PDL (Willner *et al*. 2004). Similarly in Figure 6.16 (c) the high PMD influenced the PDL thereby leading to its deviation from the Maxwellian PDF as represented by the areas not populated by the PDL values.

It can be seen from Figure 6.16 that the addition of components increases PDL in the link as represented by the tail of the Maxwellian PDF on the right side of each graph. This has been observed previously in section 6.6 and section 6.7. Similar observations have been found by Corsi *et al*. (1998), El Amari *et al.* (1998) and Damask *et al*. (2002) and Fukada (2002) where they used the PDF to predict the global PDL of concatenated components and fibres. The Maxwellian PDF was applied on the PDL data in Figure 6.16 following the work of Lu et al. (2001) where they considered the interaction between PDL and PMD values.

6.7.3. Determination of PMD from PDL data

It is understood that the presence of PMD in a link having PDL results in the PDL changing with wavelength (Gisin and Huttner, 1997). This phenomenon can be used to obtain information related to PMD from measured PDL data.

In order to investigate the strength of the PMD in a PDL link, measurements were carried out with constant PDL and for each component and with varying PMD. The frequency of PDL fluctuations depends on the PMD value. The larger the PMD value, the higher the fluctuation frequency. The corresponding wavelength dependence of the PDL can be seen in Figure 6.17. In Figure 6.17, where a splitter and three single mode buried fibres all of the same average PDL values (0.2 dB) and different PMD values were selected and plotted. It can be seen in Figure 6.17 that the PDL varies gradually with wavelength. The highest fluctuation rate of PDL is observed for highest values of PMD as given by the element having PMD of 5.45 ps in Figure 6.17.

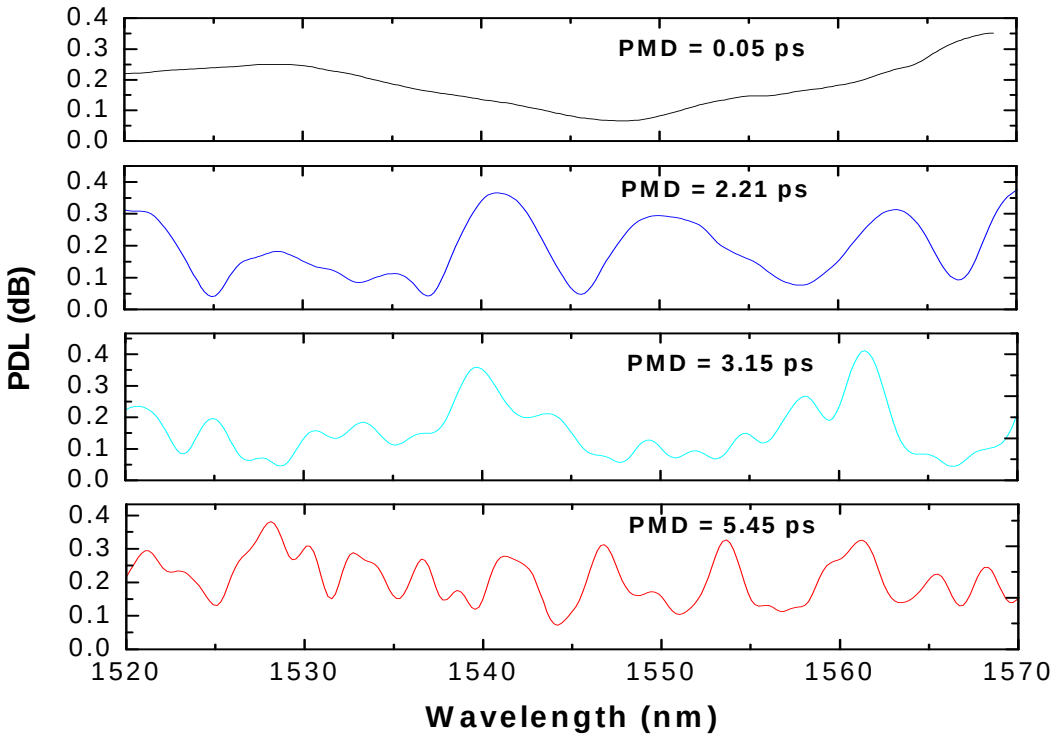

Figure 6.17: Various PDL spectra for different values of PMD.

The birefringence within sections of single mode fibre varies randomly along the length of the fibre and this affects the state of polarization (SOP) as the wavelength is varied. This was explained in the previous sections. Since a splitter with lower PMD value has fairly low birefringence, the PDL change as the wavelength is continuously varied is minimal in fluctuations. High PMD results in high birefringence which results in more rapid fluctuations of PDL changing with wavelength.

The results in Figure 6.17 should not be confused with the results in Figure 6.13, where a birefringent PM fibre was equally spliced to generate a randomly coupled device, resulting in a decrease in PMD as discussed in section 6.7.1.

To obtain the PMD information from the PDL data, a fast Fourier transform (FFT) of the PDL data is applied. A Gaussian is fitted to the curve and by determining its width, the PMD information is obtained. This method is based on the fact that a PDL element in a PMD environment becomes a statistical quantity, varying with the wavelength. This is because sections of fibre present different magnitudes of birefringence which cause changes in polarization states as the wavelength is varied.

Figure 6.18 (a) and (b) show PDL as a function of wavelength and the Fast Fourier Transform (FFT) of (a), respectively. A PMD value of 2.979 ps is measured using the JME method, as noted in Figure 6.18 (a). From the PDL data, a FFT plot is generated and a Gaussian curve is applied (Figure 6.18 (b). The width of the Gaussian fit is used to infer information on PMD. In this case the obtained PMD from the FFT method is 2.997 ps as shown in Figure 6.18 (b). Very good correlation of the two PMD values is obtained. Further discussion on the FFT technique can be obtained from El Amari *et al*. (1998). From this source the same procedure as above is followed. This method is applicable for both negligible and non-negligible polarization mode coupling.

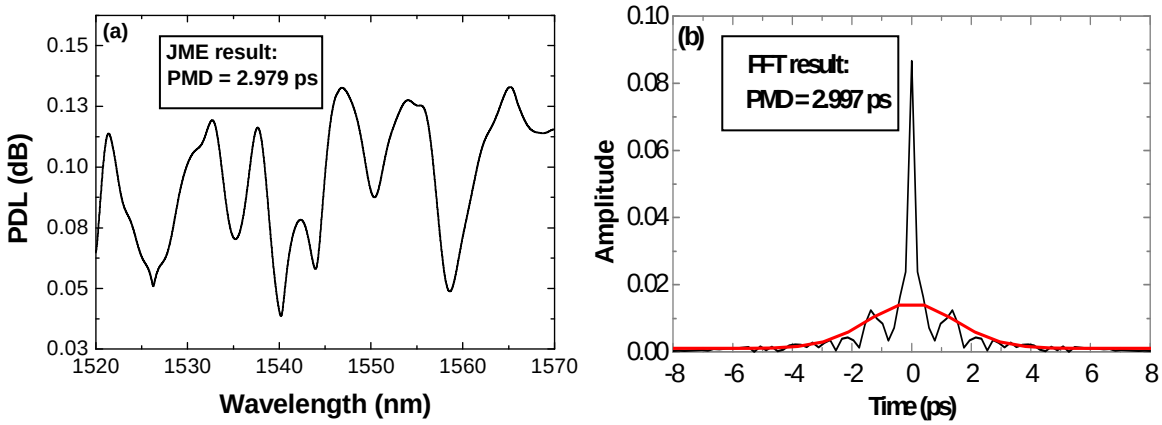

Figure 6.18: (a) PDL versus wavelength and (b) FFT of the PDL signature for the case of a concatenation of a PMD and a PDL element

From Figure 6.18 (a) the changing of PDL with wavelength as already discussed in the previous sections is influenced by PMD which is caused by birefringence within sections of fibre and the PDL element.

We performed similar measurements of PMD on other systems; and table 6.2 summarises these results. It can be seen from table 6.2 that the results for the JME and FFT methods compare very well. The standard deviation for the PMD determined from the FFT method appears to be higher than when using the JME method. We believe this could be attributed to the applied Gaussian fit to the PDL data. Note that the central (autocorrelation) peak carries no further information related to the PMD.

Table 6.2: PMD values obtained from the JME and the FFT of the PDL data

Device	PMD from JME (ps)	PMD from FFT (ps)
50:50 1×2 splitter	0.050 ± 0.005	0.062 ± 0.020
Isolator	0.135 ± 0.002	0.137 ± 0.080
Attenuator	1.113 ± 0.011	1.126 ± 0.180
Single mode fibre1	2.979 ± 0.021	2.997 ± 0.233
Single mode fibre2	7.008 ± 0.341	7.142 ± 0.642

6.7.4. Long term PDL and PMD measurements

In this section PMD and PDL results obtained from the laboratory and buried single mode fibre are presented and analyzed. This comprises a 24.74 km single mode fibre (wound on a shipping spool in the laboratory) and 28.8 km single mode buried cable (deployed in Port Elizabeth). The wavelength range was scanned between 1520 to 1570 nm with a step size of 0.2 nm and the PDL and PMD measured with the JME method. Note that the length of each fibre was confirmed using a standard optical time domain reflectometer (OTDR).

Figure 6.19 (a) and (b) show the contour map of the measured PDL and DGD (average DGD gives PMD) as a function of wavelength and time for the single mode fibre spool. Both PDL and DGD vary slowly with time and wavelength.

In Figure 6.19 (a) the small changes of PDL (step size of 0.05 dB) with wavelength and time can be thought to be influenced by the changing DGD. This is because sections of single mode fibre induce random birefringence (mode coupling) which change the polarization states as the wavelength is varied resulting in PDL changing with wavelength. On the other hand, temperature changes can induce birefringence and this can result in mode coupling angles varying along the length of the fibre. These variations (birefringence and mode coupling) cause PDL/DGD to change with wavelength.

In Figure 6.19 (b) the DGD changes with wavelength (step size 0.02 ps) and vary slowly with time. During measurements the DGD changes with wavelength is attributed to different magnitudes of birefringence within sections of single mode fibre.

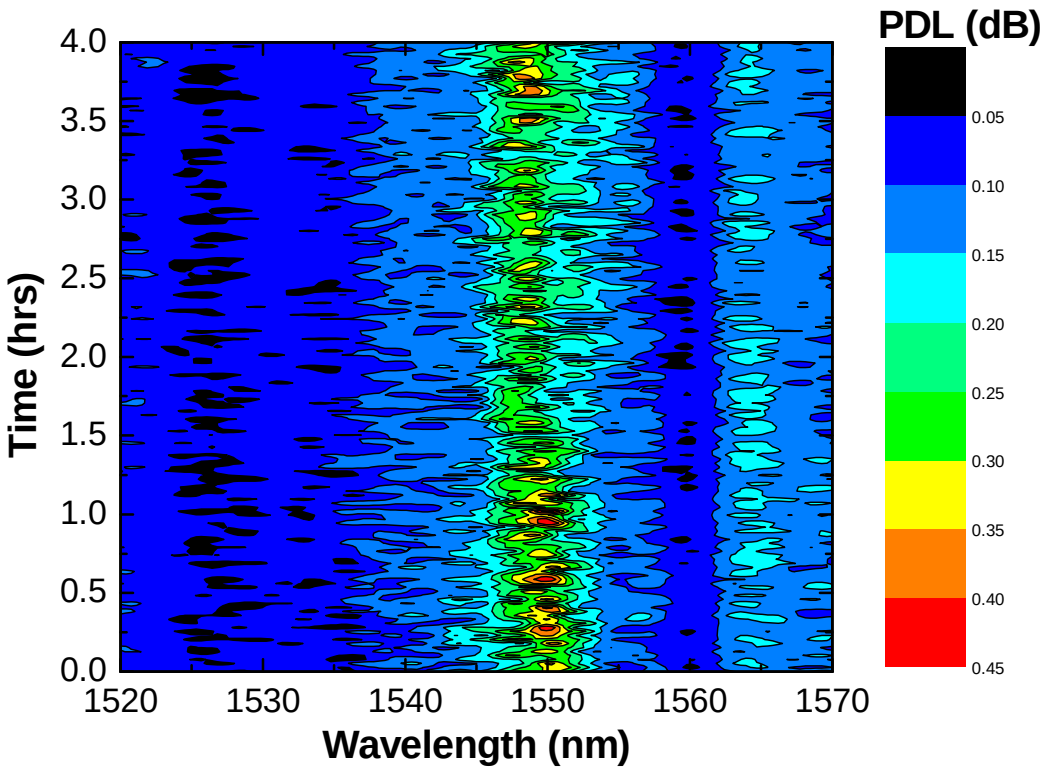

(a)

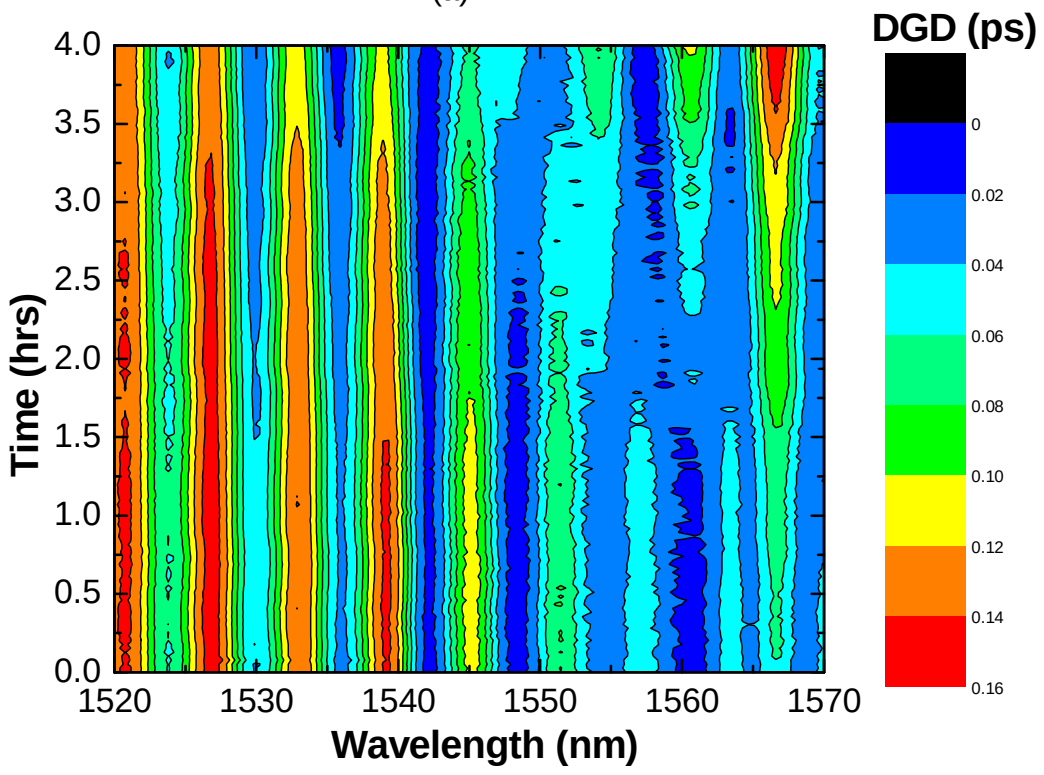

(b)

Figure 6.19: Contour plots of the (a) PDL and (b) PMD for the 24.74 km spool of fibre.

DGD change with time is attributed to induced temperature change that varies birefringence within sections of single mode fibre.

Figure 6.20 (a) and (b) show the colour map of PDL and DGD for the buried link respectively.

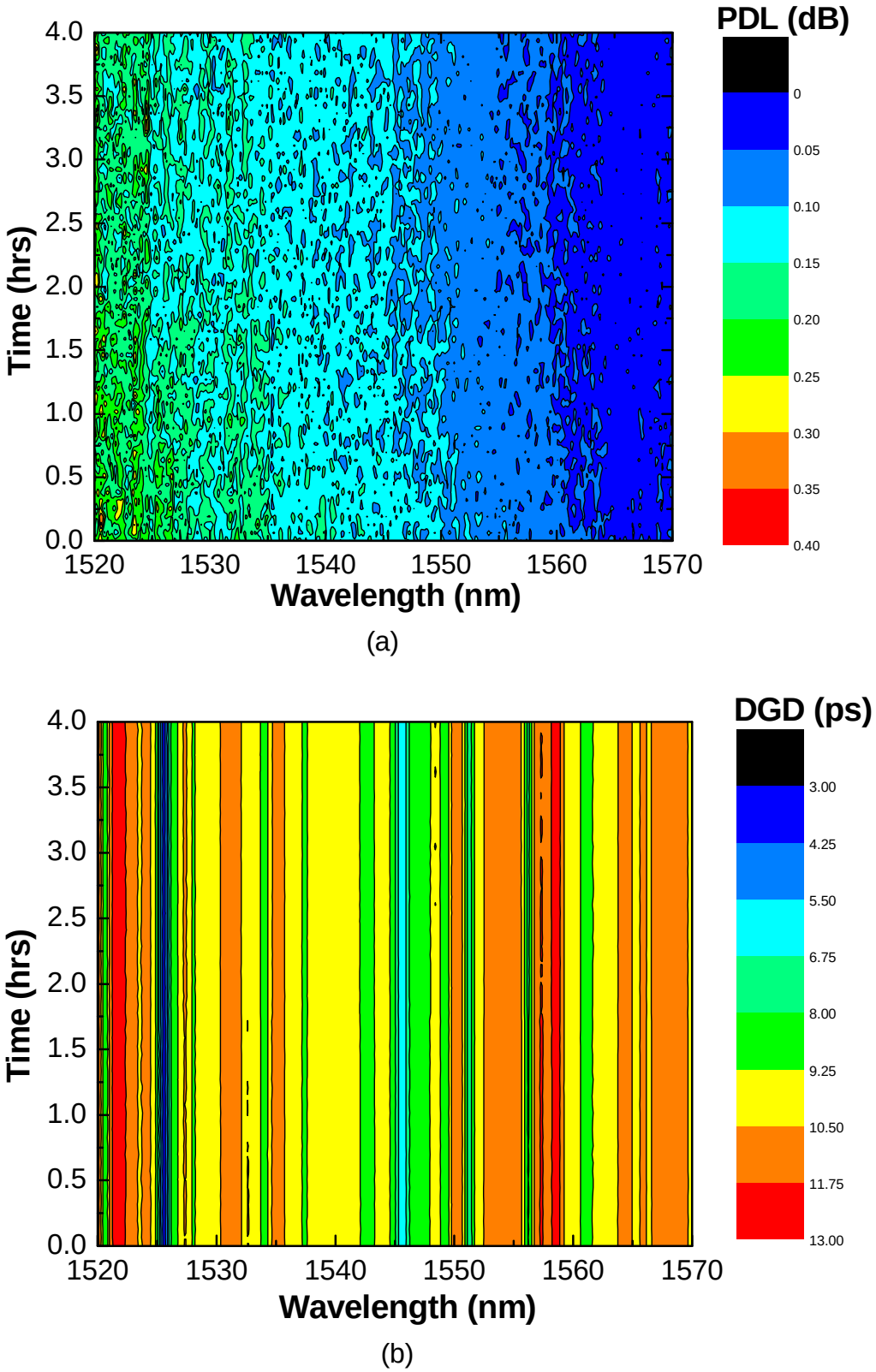

Figure 6.20: Contour plots for buried single mode fibre (28.8 km) with (a) PDL and (b) DGD as function of time and wavelength.

A step size of 0.05 dB is chosen for the PDL measurements. The PDL changes in Figure 6.20 (a) could be attributed to the changing birefringence within sections of single mode fibre which result in mode coupling sites as previously discussed. The birefringence changes the output SOPs as the wavelength is varied and the resultant is PDL changing with wavelength. In addition, variation in temperature can induce different magnitude of birefringence leading to changes in polarization states. Certain output SOPs will be attenuated more than the others and the difference between the maximum and minimum output SOPs generate the worst PDL cases are observed as shown for both Figures 6.19 and 6.20. In addition, the JME method is highly sensitive to any variations since one measure SOPs and we believe this could be an effect that influenced the observed minor changes in DGD and PDL for both figures.

In using a step size of 0.02 ps in Figure 6.20 (b) similar to Figure 6.19 (b), the change of DGD with time was observed (not shown) though it cannot be seen for a step size of 1.25 ps. The change of DGD with time is attributed to the temperature change at the junctions (sites that are not buried-connection sites) where the fibre is exposed to the environment. We believe that these parts suffer small DGD changes due to the environmental perturbations (in this case temperature) as already discussed which induces varying birefringence within single mode fibre and therefore resulting in the observed DGD change with wavelength.

The DGD and PDL results for the laboratory showed a significant change of time and wavelength. The reason as previously discussed was attributed to the random birefringence within sections of single mode fibre. The buried fibre also showed PDL and DGD measurements changing with time and wavelength. The DGD change with time was very small even selecting a step size of 0.02 (not shown). The reason could be due to the fact that for a buried link, the temperature variations were not as significant as for the laboratory measurements. To the best of our knowledge, these results are the first studies of this type and further studies are to be conducted in order to identify any.

6.8. Effect of PMD/PDL on the BER

The rate at which errors occur in telecommunication networks is one of the most important parameters to be measured. These errors mainly result at high bit rates (≥ 10 Gb/s) with the common cause being polarization mode dispersion (PMD) and polarization dependent loss (PDL). In this section a fibre link suffering from the effects of PDL and PMD is simulated and the bit error rate (BER) determined using Virtual Photonics Transmission Maker 7.5. A simulated environment is important since other parameters that might influence BER apart from PMD and PDL can be eliminated as compared to experimental work where elimination of these effects is not easy. Also, this software is used to generate the eye diagram which is used to show how the transmitted signal is distorted by the effects of PDL and PMD. The eye diagram is a superposition of pseudorandom patterns consisting of zeros and ones of the transmitted bits.

Figure 6.21 shows the schematic diagram used in the simulation to determine the bit error rate and the eye diagram.

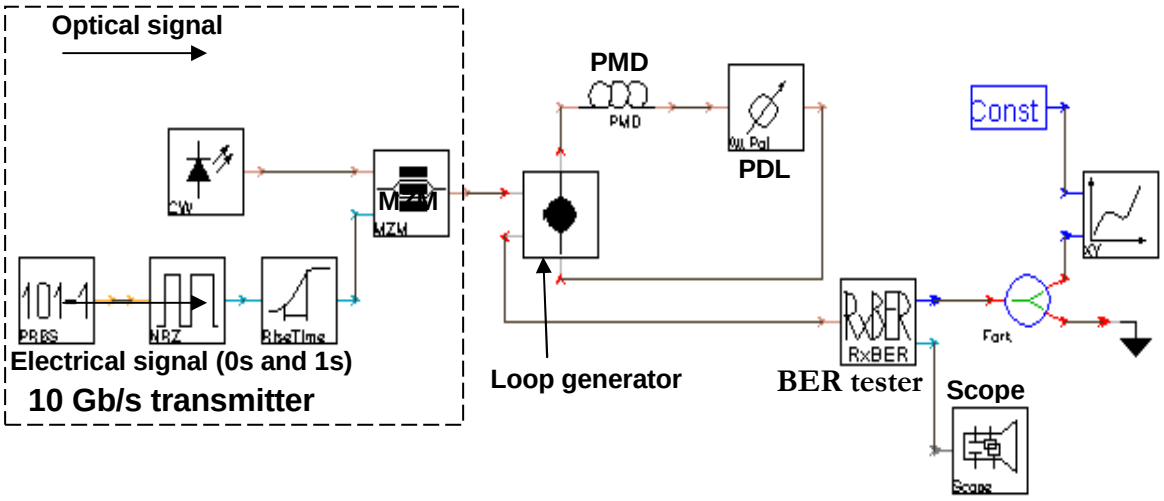

Figure 6.21: System simulation to show the effect of PMD and PDL on BER

An electrical signal generating 10 Gb/s electrical pulses with pseudorandom bit sequence (PRBS) and non-return to zero (NRZ) format is used to modulate an optical signal from a continuous wave laser source with an electrooptic lithium niobate Mach-Zehnder modulator (MZM). This forms the transmitter of the simulated transmission network.

The input Y junction in the MZM splits the input signal equally between the upper and lower waveguides and the output Y junction then combines the two signals. The signals can combine constructively or destructively depending on the optical path difference between the two branches. The refractive index between the waveguides is changed by the electric field induced by an applied voltage. Therefore by varying the voltage from maximum to minimum the output signal is modulated. The modulated signal is then fed to the loop generator that specifies the number of PMD and PDL components in the link.

The PMD is represented by a single mode fibre and the PDL by the polarization attenuator, which preferentially attenuates one of its polarization axes. The PDL of the fibre was considered negligible in comparison to the PDL of an attenuator. The BER tester is represented by RxBER. The scope displays the eye diagram. Figure 6.22 shows a schematic diagram used to determine the PMD and PDL of the link using the Jones matrix. Note that the transmitter is represented as a Jones matrix generator while the receiver is represented by a Jones matrix analyzer.

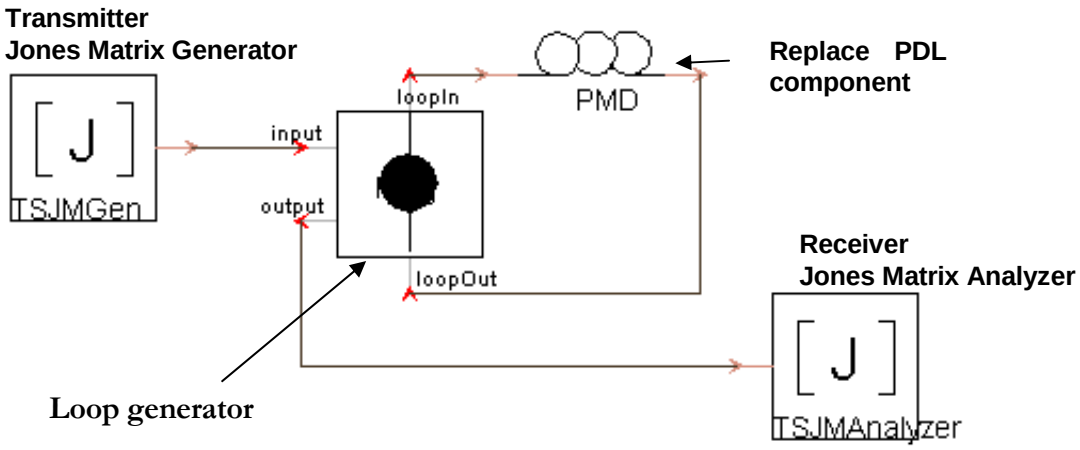

Figure 6.22: Schematic diagram in VPI Transmission maker 7.5 showing how PMD and PDL is determined using the Jones matrix method. The PMD fibre can be substituted with PDL components for PDL measurements.

Simulation measurements were conducted on a link affected by PMD and PDL using the following parameters: The optical laser was set at 3 mW to provide enough power to the receiver and we generated 32768 (2^{15}-1 bit length) pseudorandom bit sequence (PRBS) bits at a transmission rate of 10 Gb/s. The transmission line had an overall length of 100 km. To make sure that the link

consisted of only PMD and PDL, all non-linear effects were nulled. Figure 6.23 shows the simulated BER in a link with PMD and PDL.

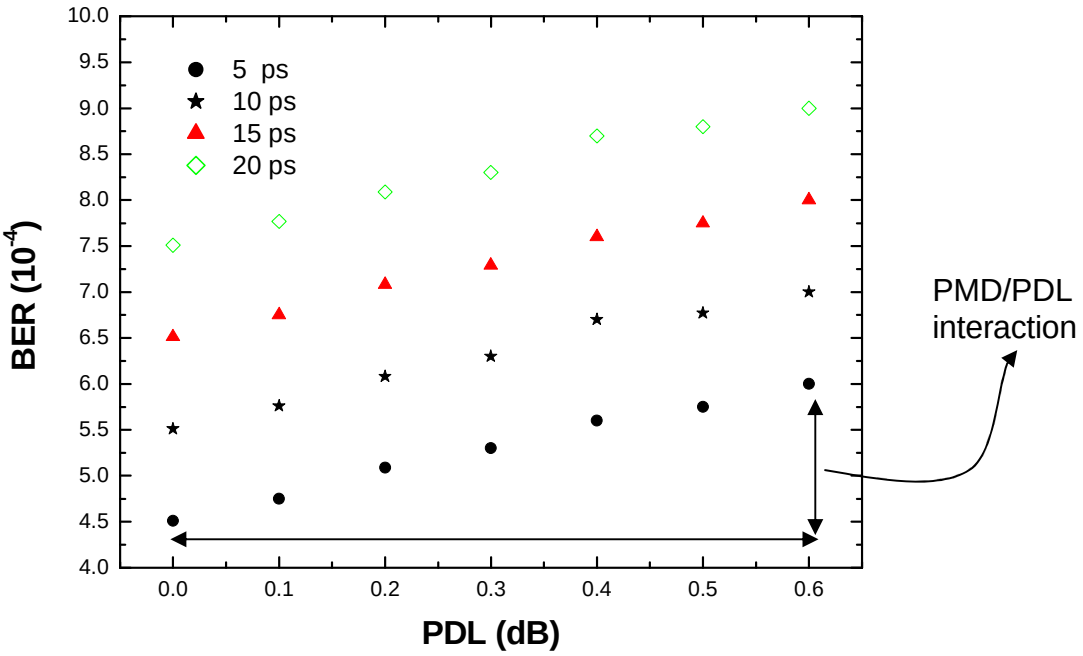

Figure 6.23: The variation of BER with PMD and PDL

It can be seen that the BER increases with both PMD and PDL. The arrows in Figure 6.23 indicate the effect of PMD and PDL interaction. A similar trend has been observed by Kim *et al*. (2002) and they also found this increase of BER with both PMD and PDL.

In telecommunication systems, eye diagrams are efficient in evaluating system performance. The effects of PMD and PDL are easily recognised through visualizing the eye diagrams. The eye diagrams corresponding to PDL values of 0 and 3 dB and PMD values of 0 and 1.5 ps were generated as represented in Figure 6.24. The large part of the eye represented by a shaded area called the open area means that the effects of PDL and PMD are set to zero. This is represented by Figure 6.24 (a). A 3 dB PDL is added and the upper section of the eye is starting to be distorted (interference in the transmitted bits) and this is also indicated by the reduction of the shaded part of the open area. This is represented in Figure 6.24 (b).

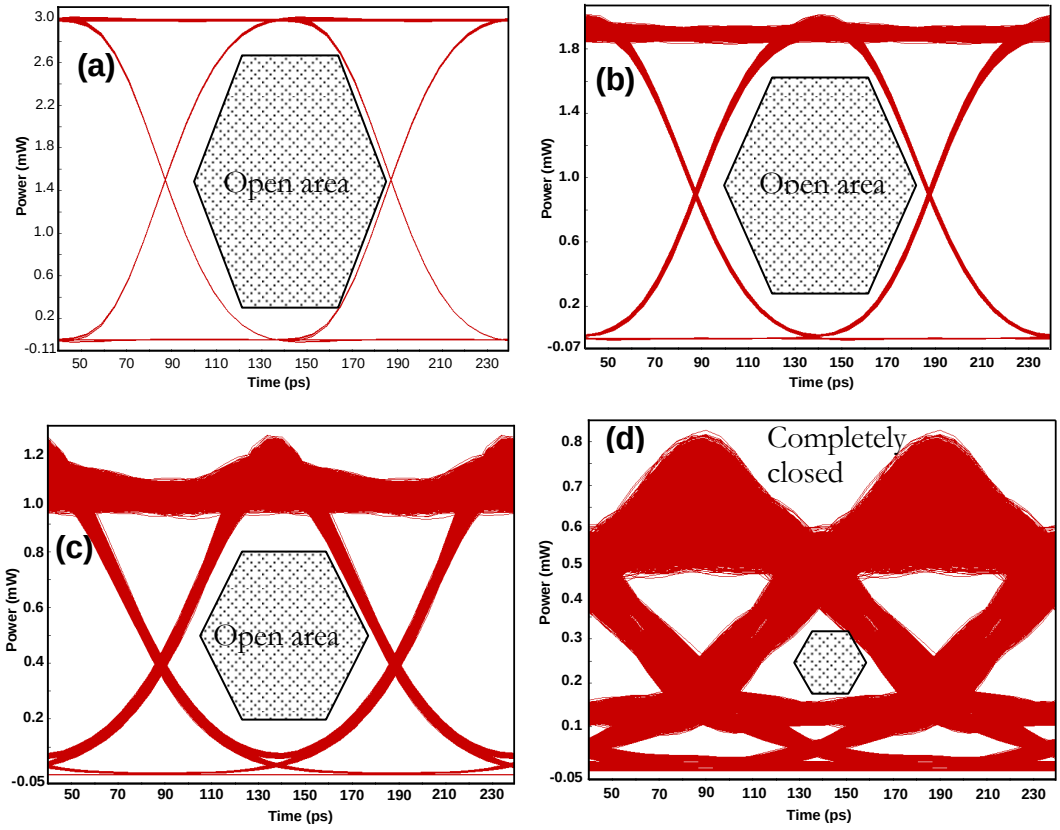

Figure 6.24: Eye diagrams for cases (a) no PMD and PDL effects (b) PDL of 3 dB and 0 ps PMD, (c) PDL of 0 dB 1.5 ps PMD and (d) PDL of 3 dB and 1.5 ps PMD with different size of the open area for the eye.

It can be seen that 1.5 ps PMD results in a highly distorted eye as represented by Figure 6.24 (c) and again the shaded area is reduced further. Both PDL (3 dB) and PMD (1.5 ps) in a link leads to a distorted eye which results in a complete closure of the eye as represented in Figure 6.24 (d), where the open area has been reduced to its smallest shape. It can be seen that both PMD and PDL degrade the system more than either PMD or PDL alone as represented by Figure 6.24 (d). This is well known theoretically. We have analyzed the effects of polarization mode dispersion and polarization dependent loss in high speed transmission systems. As both PMD and PDL increase the bit error rate increases. This has been identified as the limiting factor at high bit rate transmission systems. It is therefore important to consider the combined effects of PDL and PMD.

In summary, in this chapter we have shown how PDL measurements of various components were characterized using the three different techniques and PDL results of three techniques compared very well. The interaction between PMD and PDL and the wavelength dependence of PDL due to the presence of PMD were investigated. In addition, PMD was extracted from the PDL data following the fluctuation of PDL with wavelength due to the presence of PMD. The bit error rate in the presence of both PMD and PDL was characterized and it was shown that both effects lead to high BER values.

CHAPTER 7

CONCLUSIONS

One of the purposes of this study was to investigate and assess PDL on different components using three PDL measurements techniques, namely, the Jones matrix eigenanlysis (JME) method, polarization scrambling method and optical spectrum analyzer (OSA) method both in the laboratory and on deployed optical fibre transmission links. The combined effects of PDL and PMD were investigated in relation to the wavelength dependence of PDL, the bit error rate (BER) and the eye diagrams. Furthermore, the PMD was determined for different components using the PDL data.

In terms of experimental findings presented in this dissertation, Chapter 6 contains PDL results of various components and fibre. The PDL results over a wavelength range are presented. The results show that PDL varies as the wavelength changes. The PDL change with wavelength is attributed to the random SOP rotations (topological effect) within sections of connecting fibres that result in mode coupling at the junctions interlinked with components that are polarization sensitive. Each wavelength will present its own PDL value that will manifest itself as a statistical noise thereby degrading the transmitted signal. This means that compensation of PDL for each wavelength is required, especially for DWDM systems that incorporate many of the polarization sensitive components.

A comparison of PDL measurements using the three techniques was performed for various components. The PDL results from the three techniques compared very well. This further increased our confidence on PDL measurements using the three techniques.

In real optical links many PDL elements are incorporated and their relative orientation cannot be controlled due to the influence of interconnecting fibres. This requires a statistical analysis of PDL. A PDL element of the same PDL magnitude was concatenated. The mean PDL and standard deviation was considered for each concatenation. The results show that PDL increases as the components are added but the total PDL is less than the sum of each PDL element in the

concatenation. This was attributed to the fact that the polarization sensitive axes of the PDL components are misaligned relative to each other and therefore the PDL depends on the relative orientation of the PDL axes at each connection since at each connection there will be an additional PDL from each individual segment contributing to the overall/global PDL.

The combined effects of PDL and PMD were investigated using a PMD/PDL emulator. The results show that PMD decreased while PDL increased as the segments of PM fibre were joined together to generate the emulator. The decrease in the overall PMD was attributed to the induced mode coupling sites which tend to add or subtract the PMD of each individual segment of the entire length. Each segment had its own PDL value and therefore resulted in PDL increase as the segments were joined together.

For a single length of PM fibre wound around different diameters, we observed that PDL increased while PMD remain fairly constant from large to small diameters and we believe the stress induced in the PM fibre did not contribute to PMD. We therefore concluded that the increase of PDL was mainly due to the bend-induced losses.

The fluctuations of PDL in terms of different magnitude of PMD were investigated. We observed that from low to high values of PMD, the PDL fluctuations with wavelength increased. We used this observation to extract the PMD information from the PDL data. The PMD results obtained from the JME method compared very well with the PMD results from the fast Fourier transform (FFT) method.

The probability distribution of PDL is found to be a Maxwellian distribution when PDL components are considered with low values of PMD. As sections of PM fibre presenting PMD were added, the PDL increased and its distribution deviated away from the Maxwellian.

Studies on long term measurements of PDL and PMD showed that both PDL and PMD remain fairly constant with time and vary slowly with wavelength for deployed buried cables and spooled laboratory fibres. This was attributed to the fact that the

environmental perturbations such as wind and vibration were minimized which leaves temperature alone to be the main dominant factor.

The bit error rate (BER) was characterized for the link affected by both PDL and PMD. We observed that the BER increased linearly as the PDL and PMD values were increased. This was attributed to the induced birefringence in optical fibres and polarization sensitive components which will therefore lead to optical pulse spreading and consequently high signal fluctuations degrading the signal to noise ratio (SNR). On the other hand, the eye diagrams show a distorted signal when considering both PDL and PMD as opposed to the less distorted signal from each effect alone.

Finally, this study has shown the importance of considering both PDL and PMD for an optical fibre link operating at high bit rates. For future work it is suggested that further modelling techniques be investigated to evaluate the combined effects of PDL and PMD specifically on the BER, optical signal to noise ratio (OSNR) and outage probabilities. Consideration should also be given to the design of a PMD/PDL compensator, as this will be necessary to reduce the combined effects of PDL and PMD in future.

APPENDIX

RESEARCH OUTPUTS OF THE AUTHOR

2007

G. Pelaelo, L. Wu, A.W.R. Leitch and V. Musara, "*Characterization of polarization dependent loss in optical fibres and components in the presence of polarization mode dispersion*", Oral presentation at the 52nd South African Institute of Physics (SAIP) Conference, Johannesburg, South Africa, 3-6 July 2007.

2006

G. Pelaelo, L. Wu, D. Waswa and A.W.R Leitch, "*Investigation of polarization dependent loss in optical components and various optical components*", Poster presentation at the 51st South African Institute of Physics (SAIP) Conference, Western Cape, South Africa, 3-7 July 2006.

REFERENCES

Application Note[1]: Gunnar Stolze, Stefan Rathgeb, and Markus Maile, “Optical All-Loss Test Solution”, Agilent Technologies, 1997.

Application Note[2], “Polarization Dependent Loss Measurement of Passive Optical Components”, Agilent Technologies, 1999.

M. Boroditsky, M. Brodsky, N. J. Frigo, P. Magill and J. Evankow, “Viewing Polarization Strings on Working Channels: High-Resolution Heterodyne Polarimetry”, Proc*. European Conference on Optical Communications (ECOC)*, Stockholm, Sweden (We1.4.5), 2004.

CEI/IEC TR 61282-3, “Fibre optic communication system design guides-part 3: Calculation of polarization mode dispersion”, First edition, 2002.

L. Chen, J. Cameron and X. Bao, “Statistics of polarization mode dispersion in presence of the polarization dependent loss in single mode fibers”, *Optical Communications*, vol. 169, pp. 69-73, 1999.

L. Chen, and X. Bao, “Polarization-Dependent Loss-Induced Pulse Narrowing in Birefringent Optical Fiber with Finite Differential Group Delay”, *Journal of Lghtwave Technology*, vol. 18, no. 5, pp. 665-667, 2000.

L. Chen, O. Chen, S. Hadjifaradji and X. Bao, “Polarization mode dispersion measurement in system with polarization dependent loss or gain”, *IEEE Photonics Technology Letters*, vol. 16, no. 1, pp. 206-208, 2004.

L. Chen, Z. Zhang and X. Bao, “Polarization dependent loss vector measurement in a system with polarization mode dispersion”, *Optical Fiber Technology*, vol. 12, pp. 251-254, 2005.

P. C. Chou, J. M. Fini and H. A. Haus, “Real-Time Principal State Characterization for use in PMD Compensators”, *IEEE Photonics Technology Letters*, vol. 13, no. 6, pp. 568-570, 2001.

P. C. Chou, J. M Fini and H. A. Haus, “Demonstration of a *Feed-Forward* PMD Compensation Technique”, *IEEE Photonics Technology Letters*, vol. 14, no. 2, pp. 161-163, 2002.

F. Corsi, A. Galtarossa and L. Palmieri, “Polarization mode dispersion characterization of single-mode optical fiber using backscattering technique”, *Journal of Lightwave Technology*, vol. 16, no. 10, pp. 1832-1843, 1998.

R. M. Craig, ”Accurate Spectral characterization of polarization dependent loss”, *Journal of Lightwave Technology*, vol. 21, no. 2, pp. 432-437, 2003.

R. M. Craig, S. L. Gilbert and P. D. Hale, “High-resolution, nonmechanical approach to polarization-dependent transmission measurements”, *Journal of Lightwave Technology*, vol. 16, no. 7, pp. 1285-1294, 1998.

N. Cyr, A. Girard and G. W. Schinn, “Stokes parameter analysis method, the consolidated test method for PMD measurements”, *in Proceedings of the National Fibre Optical Engineering Conference*, Chicago IL, p. 280, 1999.

N. Cyr, “Method and apparatus for measuring polarization mode dispersion of optical devices”, U.S. Patent 6,204,924, 2001.

A. O. Dal Forno, A. Paradisi, R. Passy and J. P. von der Weid, “Experimental and theoretical modeling of polarization mode dispersion in single mode fibres”, *IEEE Photonics Technology Letters*, vol. 12, pp. 296-298, 2000.

J. N. Damask, ”Polarization Optics in Telecommunication”, *Springer series in Optical sciences*, vol. 101, pp. 371-379, 2005.

J. N. Damask, “Programmable polarization mode dispersion generation”, in Tech. Digest, *Symposium on Optical Fiber Measurements* (SOFM 2002), Boulder, CO, 2002.

D. Derickson (editor), “Fibre Optic Test Measurement”, Prentice Hall, 1998.

P. Ding and J. Sun, “Polarization-mode dispersion influenced by polarization-dependent loss and chirp for a Gaussian pulse”, *Optical Engineering*, vol. 46, no. 5, pp. 1-3, 2007.

A. B. dos Santos and J. P. von der Weid, “PDL effects in PMD emulators made out with HiBi fibers: Building PMD/PDL emulators”, *IEEE Photonics Technology Letters*, vol. 16, no. 2, pp. 452-454, 2004.

A. B. dos Santos, M. R. Jimenez, J. P. von der Weid and A. Djupsjöbacka, “Statistics measurements of BER fluctuations due to PMD in 10 Gb/s optical transmissions”, *IEEE Photonics Technology Letters*, vol. 14, pp. 926-928, 2002.

A. El Amari, N. Gisin, Beat Perny, H. Zbinden, and Christian W. Zimmer, “ Statistical Prediction and Experimental Verification of Concatenations of Fiber Optic Components with Polarization Dependent Loss”, *Journal of Lightwave Technology*, vol. 16, no. 3, pp. 332-339, 1998.

A. Eyal, D. Kuperman, O. Dimenstein and M. Tur, “Polarization dependence of the intensity modulation transfer function of an optical system with PMD and PDL”, IEEE *Photonics Technology Letters*, vol. 14, no. 11, pp. 1515-1517, 2002.

A. Eyal and M. Tur, “Measurement of polarization mode dispersion in systems having polarization dependent loss or gain”, *IEEE Photonics Technology Letters*, vol. 9, pp. 1256-1258, 1997.

A. Eyal and M. Tur, “A modified Poincare sphere technique for the determination of polarization-mode dispersion in the presence of differential gain/loss”, in Tech. Dig., *Optical Fiber Communications Conference (OFC’98),* San Jose, CA, 1998, paper ThR1, p. 340.

D. L. Favin, B. M. Nyman and G. M. Wolter, “System and method for measuring polarization dependent loss”, U.S. Patent 5,371,597, 1994.

X. Fu, M. O’Sullivan and J. Goodwin, “Equivalent First-Order Lumped-Elements Model for Networks with Both PMD and PDL”, *IEEE Photonics Technology Letters*, vol. 16, no. 3, pp. 939-941, 2004.

Y. Fukada, “ Probability Density Function of Polarization Dependent Loss (PDL) in Optical Transmission System Composed of Passive Devices and Connecting Fibers”, *Journal of Lightwave Technology Letters*, vol. 20, no. 6, pp. 953-964, 2002.

A. Galtarossa, G. Gianello, C. G Someda and M. Schiano, “In Field Comparison among polarization mode dispersion measurements techniques”, *Journal of Lightwave Technology*, vol. 14, no. 1, pp. 42-49, 1996.

A. Galtarossa, L. Palmieri, A. Pizzinat, M. Schiano and T. Tambosso, “Measurement of local beat length and differential group delay in installed single mode fibers,” *Journal of Lightwave Technology*, vol. 18, no. 10, pp. 1389-1394, 2000.

T. B. Gibbon, “Polarization mode dispersion compensation in an optical fibre”, PhD Thesis, *Nelson Mandela Metropolitan University*, South Africa, 2007.

N. Gisin and J. P. Pellaux, “Polarization mode dispersion: Time versus frequency domains”, *Optics Communications*, vol. 89, pp. 316-323, 1992.

N. Gisin, “Statistics of Polarization Dependent Losses”, *Optics Communications*, vol. 114, pp. 399-405, 1995.

N. Gisin and B. Huttner, “Combined effects of polarization mode dispersion and polarization dependent losses in optical fibres”, *Optics Communications*, vol. 142, pp. 119-125, 1997.

N. Gisin, B. Huttner and N. Cyr, ”Influence of polarization dependent loss on birefringent optical fiber networks”, *Optical Fiber Communications*, 2000.

N. Gisin, R. Passy and J. P. der Weid, “Definitions and Measurements of Polarization Mode Dispersion: Interferometric Versus Fixed Analyzer Methods”, *IEEE Photonics Technology Letters*, vol. 6, no. 6, pp. 730-732, 1994.

S. Harris and D. Ives, “Polarization Mode Dispersion in Restricted Optical Bandwidth: An Evaluation of Measurement Techniques”, NPL Report CETM 40, ISSN 1467-3932, 2002.

M. C. Hauer, Q. Yu, A. E. Willner, E. R. Lyons, C. H. Lin, A. A. Au and H. P. Lee, “Compact, all-fiber PMD emulator using an integrated series of thin film micro heaters”, *Proceedings Optical fiber Communications (OFC)* 2002, Anaheim, CA, pp. 374-375, 2002.

H. F. Haunstein and H. M. Kallert, “Influence of PMD on the performance of optical transmission systems in the presence of PDL”, Optical Fiber Conference, OFC 2001, vol. 3, pp. 4.1- 4.3, 2001.

B. L. Heffner, “Automated measurement of polarization mode dispersion using Jones matrix eigenanalysis,” *IEEE Photonics Technology Letters*, vol. 4, no. 9, pp. 1066-1068, 1992.

B. L. Heffner, “Accurate, Automated Measurement of Differential Group Delay Dispersion and Principal State Variation using Jones Matrix Eigenanalysis”, *IEEE Photonics Technology Letters,* vol.5, no. 7, pp. 814-817, 1993.

B. Huttner, C. Geiser and N. Gisin, “Polarization-Induced Distortions in Optical Fiber Networks with Polarization-Mode Dispersion and Polarization-Dependent Losses”, *IEEE Journal of Selected Topics in Quantum Electronics*, vol. 6, no. 2, pp. 317-329, 2000.

IEC 61300-3-2, “Fibre optic interconnecting devices and passive components - Basic test and measurements procedures – Part 3-2: Examinations and measurements – Polarization dependence of attenuation in a single-mode fibre optic device”, International Electrotechnical Commission Std., 1999.

IEC/CEI 60793-1-48, “Measurement methods and test procedures-Polarization mode dispersion”, part 1-48, 2007.

I. P. Kaminow, “Polarization in Optical fibres”, *IEEE Journal of Quantum Electronics*, vol. 17, no. 1, pp. 15-22, 1981.

M. Karlsson, J. Brentel, and P. A. Andrekson, “Long term-Term Measurement of PMD and Polarization Drift in Installed Fibres”, *Journal of Lightwave Technology*, vol. 18, no. 7, pp. 941-951, 2000.

M. Karlsson and M. Petersson, “Quaternion Approach to PMD and PDL Phenomena in Optical Fiber Systems”, *Journal of Lightwave Technology*, vol. 22, no. 4, pp. 1137-1146, 2004.

G. Keiser, “*Optical Fiber Communications*”, McGraw-Hill, 2000.

J. Kim and Richard Buerli, “An Evaluation of Polarization dependent loss-characterization methods”, *Journal of Lightwave Technology*, vol. 17, no. 9, pp. 1-9, 2000.

H. Kim, S. Kim, S. Hwang and Y. Oh, “Impact of Dispersion, PMD, and PDL on the Performance of Spectrum-Sliced Incoherent Light Sources Using Gain-Saturated Semiconductor Optical Amplifiers”, *Journal of Lightwave Technology*, vol. 24, no. 2, pp. 775-785, 2006.

N. Y. Kim, D. L. Lee, H. Yoon, J. Park and N. Park, “Limitation of PMD Compensation Due to Polarization-Dependent Loss in High-Speed Optical Transmission Links”, *IEEE Photonics Technology Letters*, vol. 14, no. 1, pp. 104-106, 2002.

D. Kuperman, A. Eyal, O. Mor, S. Traister and M. Tur, “Measurement of the Input States of Polarization That Maximize and Minimize the Eye Opening in the Presence of PMD and PDL”, *IEEE Photonics Technology Letters*, vol. 5, no.10, pp. 1425-1427, 2003.

Y. Li and A. Yariv, “Solutions to the dynamical equation of polarization-mode dispersion and polarization-dependent losses”, *Journal of Optical Society of America. B*, vol. 17, no. 11, pp. 1821-1827, 2000.

X. Liu, C. R. Giles, X. Wei, A. J. Van Wijngaarden, Y. H. Kao, C. Xie, L. Möller and I. Kang, “Demonstration of Broad-Band PMD Mitigation in the Presence of PDL Through Distributed Fast Polarization Scrambling and Forward-Error Correction”, *IEEE Photonics Technology Letters*, vol. 17, no. 5, pp. 1109-1111, 2005.

P. Lu, L. Chen and X. Bao, “Statistical Distribution of Polarization-Dependent Loss in the Presence of Polarization-Mode Dispersion in Single-Mode Fibers”, *IEEE Photonics Technology Letters*, vol. 13, no. 5, pp. 451-453, 2001.

P. Lu, L. Chen, and X. Bao, “System Outage Probability Due to the Combined Effect of PMD and PDL”, *Journal of Lightwave Technology*, vol. 20, no. 10, pp. 1805-1808, 2002.

A. Meccozi and M. Shtaif, “The statistics of polarization-dependent loss in optical communication systems”, *IEEE Photonics Technology Letters*, vol. 14, no. 3, pp. 313-315, 2002.

C. Menyuk, D. Wang and A. Pilipetskii, “Repolarization of polarization scrambled optical signals due to polarization dependent loss”, *IEEE Photonics Technology Letters*, vol. 9, pp. 1247-1249, 1997.

Y. Namihira, K. Nakajima and T. Kawazawa, “Fully Automated Interferometric PMD Measurements for Active EDFA, Fibre Optic Components and Optical Fibres”, *Electronic Letters*, vol. 29, no. 18, pp. 1649-1650, 1993.

R. Noé, D. Sandel, M. Yoshida-Dierolf, S. Hinz, V. Mirvoda, A. Schöpflin, C. Glingener, E. Gottwald, C. Sheerer, G. Fischer, T. Weyrauch and W. Haase, "Polarization mode dispersion compensation in single-mode fibre at 10, 20, and 40 Gb/s with various optical equalizers", *IEEE Journal of Lightwave Technology* , vol. 17, pp. 1602-1616, 1999.

C. D. Poole and D. L. Favin, "Polarization-Mode Dispersion Measurements Based on Transmission Spectra Through a Polarizer", *Journal of Lightwave Technology*, vol. 12, no. 6, pp. 917-929, 1994.

C. D. Poole and R. E. Wagner, "Phenomenological Approach to Polarization Dispersion in Long Single-Mode fibres", *Electronics Letters*, vol. 22, no. 19, pp.1029-1030, 1986.

M. Shtaif and A. Meccozzi, "Polarization-Dependent Loss and Its Effect on the Signal-to-Noise Ratio in the Fiber-Optic Systems", *IEEE Photonics Technology Letters*, vol. 16, no. 2, pp. 671-673, 2004.

M. Shtaif and O. Rosenberg, "Polarization-Dependent Loss as a waveform-Distorting Mechanism and Its Effect on fiber-Optic Systems", *Journal of Lightwave Technology*, vol. 23, no. 2, pp. 923-930, 2005.

W. Shieh and S. D. Dods, "Robustness of Polarization-Mode-Dispersion Compensation in the Presence of Polarization-Dependent Loss," *IEEE Photonics Technology Letters*, vol. 17, no. 3, pp. 574-575, 2005.

A. Sivasubramanian, and V. C. Ravichandran, "Pulse narrowing in optical fiber with polarization mode dispersion and polarization-dependent loss for different input states of polarization", *Optical Engineering*, vol. 46, no. 2, pp. 025010-1-025010-5, 2007.

Y. Suetsugu, T. Kato and M. Nishimura, "Full characterization of polarization mode dispersion with random mode coupling in single mode optical fibres", *IEEE Photonics Technology Letters*, vol. 7, no. 8, pp. 887-889, 1995.

TIA/EIA-455-157, “Measurement of Polarization Dependent Loss (PDL) of Single-Mode Fibre Optic Components”, Telecommunications Industry Association Std., 1995.

TIA/EIA-455-107, “Determination of Component Reflectance or Link/System Return Loss Using a Loss Test Set”, 2000.

TSB-141, “Polarization Dependent Loss Measurement Application Issues in Telecommunications”, RMC, TIA SC FO-4.9, PN-3-0064-A, pp. 1-10, 2003.

C. Vinegoni, M. Karlsson, M. Petersson and H. Sunnerud, “The Statistics of Polarization-Dependent Loss in a Recirculating Loop,” *Journal of Lightwave Technology*, vol. 22, no. 4, pp 968-976, 2004.

D. S. Waddy, L. Chen and X. Bao, “A dynamic polarization mode dispersion emulator,” *IEEE Photonics Technology Letters*, vol. 15, pp. 534-536, 2003.

D. S. Waddy, L. Chen, S. Hadjifaradji, and X. Bao, “High-Order PMD and PDL Emulator”, *Optical Fiber Communications*, *OFC*, vol. 2, pp. 1-3, 2004.

D. S. Waddy, L. Chen and X. Bao, “Polarization effects in aerial fibers”, *Optical Fiber Technology*, vol. 11, pp. 1-19, 2005.

D. S. Waddy, L. Chen, X. Bao and D. lL. Harris, “Statistics of Relative Orientation of Principal States of Polarization in the presence of PMD and PDL”, *Proceedings of SPIE*, vol. 5260, pp. 394-396, 2003.

D. S. Waddy, L. Chen and X. Bao, “Fast PMD and PDL Measurement of Aerial Fiber”, Optical Fiber Conference, OFC 2005, pp. 1-3, 2005.

M. Wang, T. Li and S. Jian, “Analytical theory of pulse broadening due to polarization mode dispersion and polarization dependent loss”, *Optics Communications,* vol. 223, pp. 75-80, 2003.

P. A. Williams, “Modulation phase-shift measurement of PMD using only four launched polarization states: a new algorithm”, *Electronic Letters*, vol. 35, no. 18, 1999.

A. E. Willner, S. M. Reza Motaghian Nezam, L. Yan, Z. Pan and M. C. Hauer, “Monitoring and Control of Polarization-Related Impairments in Optical Fiber Systems”, *Journal of Lightwave Technology*, vol. 22, no. 1, pp. 106-125, 2004.

C. Xie, “Pulse Distortion Induced by Polarization-Mode Dispersion and Polarization-Dependent Loss in Lightwave Transmission Systems”, *IEEE Photonics Technology Letters*, vol. 15, no. 8, pp. 1073-1075, 2003.

C. Xie and L. F. Mollenauer, “Performance Degradation Induced by Polarization-Dependent Loss in Optical Fiber Transmission Systems With and Without Polarization-Mode Dispersion”, *Journal of Lightwave Technology*, vol. 21, no. 9, pp. 1953-1957, 2003.

S. Yang, L. Chen and X. Bao, “ Wavelength dependence study on the transmission characteristics of the concatenated polarization dependent loss and polarization mode dispersion elements”, *Optical Engineering*, vol. 44, no. 11, pp. (115006) 1-5, 2005.

L. S. Yan, Q. Yu, Y. Xie and A.E. Willner, “Experimental Demonstration of the System Performance Degradation due to the Combined Effect of Polarization-Dependent loss With Polarization-Mode Dispersion”, *IEEE Photonics Technology Letters*, vol. 14, no. 2, pp. 224-226, 2002.

L. S. Yan, Q. Yu, Y. Xie and A.E. Willner, “Demonstration of In-line Monitoring and Compensation of Polarization-Dependent Loss for Multiple Channels”, *IEEE Photonics Technology Letters*, vol. 14, no. 6, pp. 864-866, 2002.

M. Yu, C. Kan, M. Lewis and A. Sizmann, “Statistics of Signal-to-Noise Ratio and Path-Accumulated Power due to Concatenation of Polarization-Dependent Loss”, *IEEE Photonics technology*, vol. 14, no. 10, pp. 1418-1420, 2002.

M. Yu, C. Kan, M. Lewis and A. Sizmann, “Statistics of polarization dependent loss, insertion loss, and signal power in optical communication systems”, *IEEE Photonics Technology Letters*, vol. 14, no. 12, pp. 1695-1697, 2002.

J.Q. Zhou, H. Dong, S. Aditya, Y. D. Gong, P. Shum, X. Guo and L. Ma, “Two-states method for polarization dependent loss measurement”, *Optical Fiber Technology*, vol. 13, pp. 139-142, 2007.